Published in final edited form as:

J Immunol. 2017 April 01; 198(7): 2772–2784. doi:10.4049/jimmunol.1600310.

Novel Adjuvant Based on the Pore-Forming Protein Sticholysin II Encapsulated into Liposomes Effectively Enhances the Antigen-Specific CTL-Mediated Immune Response

Rady J. Laborde[*,1], **Oraly Sanchez-Ferras**[*,1,2], **María C. Luzardo**[*], **Yoelys Cruz-Leal**[*], **Audry Fernández**[†], **Circe Mesa**[†], **Liliana Oliver**[†], **Liem Canet**[*], **Liane Abreu-Butin**[‡], **Catarina V. Nogueira**[§], **Mayra Tejuca**[*], **Fabiola Pazos**[*], **Carlos Álvarez**[*], **María E. Alonso**[*], **Ieda M. Longo-Maugéri**[‡], **Michael N. Starnbach**[§], **Darren E. Higgins**[§], **Luis E. Fernández**[†], and **María E. Lanio**[*]

[*]Center for Protein Studies, Faculty of Biology, University of Havana, Havana 10400, Cuba

[†]Immunobiology Division, Center of Molecular Immunology, Havana 11600, Cuba

[‡]Discipline of Immunology, Department of Microbiology, Immunology, and Parasitology, Paulista Medical School, Federal University of São Paulo, São Paulo 04023-900, Brazil

[§]Department of Microbiology and Immunobiology, Harvard Medical School, Boston, MA 02115

Abstract

Vaccine strategies to enhance $CD8^+$ CTL responses remain a current challenge because they should overcome the plasmatic and endosomal membranes for favoring exogenous Ag access to the cytosol of APCs. As a way to avoid this hurdle, sticholysin (St) II, a pore-forming protein from the Caribbean Sea anemone *Stichodactyla helianthus*, was encapsulated with OVA into liposomes (Lp/OVA/StII) to assess their efficacy to induce a CTL response. OVA-specific $CD8^+$ T cells transferred to mice immunized with Lp/OVA/StII experienced a greater expansion than when the recipients were injected with the vesicles without St, mostly exhibiting a memory phenotype. Consequently, Lp/OVA/StII induced a more potent effector function, as shown by CTLs, in vivo assays. Furthermore, treatment of E.G7-OVA tumor-bearing mice with Lp/OVA/StII significantly reduced tumor growth being more noticeable in the preventive assay. The contribution of $CD4^+$ and $CD8^+$ T cells to CTL and antitumor activity, respectively, was elucidated. Interestingly, the irreversibly inactive variant of the StI mutant StI W111C, encapsulated with OVA into Lp, elicited a similar OVA-specific CTL response to that observed with Lp/OVA/StII or vesicles encapsulating recombinant StI or the reversibly inactive StI W111C dimer. These findings suggest the relative

Address correspondence and reprint requests to Prof. María E. Lanio or Dr. Luis E. Fernández, Centro de Estudio de Proteínas, Facultad de Biología, Universidad de La Habana, calle 25 entre J e I, # 455, Plaza de la Revolución, Habana 10400, Cuba (M.E.L.) or Centro de Inmunología Molecular, Avenida 15, calle 216, Atabey, Playa, P.O. Box 16040, Habana 11600, Cuba (L.E.F.). mlanio@fbio.uh.cu (M.E.L.) or luis@cim.sld.cu (L.E.F.).

ORCIDs: 0000-0002-3227-2292 (R.J.L.); 0000-0001-5308-7646 (L.O.); 0000-0003-4184-8414 (I.M.L.-M.); 0000-0002-1364-3713 (M.E.L.).

[1]R.J.L. and O.S.-F. contributed equally to this work.

[2]Current address: Goodman Cancer Research Centre and Department of Biochemistry, McGill University, Montreal, Quebec, Canada.

Disclosures

The authors have no financial conflicts of interest.

The online version of this article contains supplemental material.

independence between StII pore-forming activity and its immuno-modulatory properties. In addition, StII-induced in vitro maturation of dendritic cells might be supporting these properties. These results are the first evidence, to our knowledge, that StII, a pore-forming protein from a marine eukaryotic organism, encapsulated into Lp functions as an adjuvant to induce a robust specific CTL response.

A challenge in the field of vaccinology is the enhancement of cellular immune responses mediated by Ag-specific $CD8^+$ CTLs. Activation of naive $CD8^+$ T lymphocytes and polarization toward effective CTLs requires presentation of MHC class I–peptide complexes by APCs (signal 1), together with costimulation (signal 2) and the presence of cytokines (signal 3), such as IL-12 (1) and type I IFNs (2). Dendritic cells (DCs) are APCs that activate naive T cells (3) and process exogenous Ags for presentation to $CD8^+$ T cells. This event, termed cross-presentation, is crucial for the generation of CTLs in response to tumors or intracellular pathogens (4). Pathogen-associated molecular patterns and other signals, such as inflammatory cytokines, induce the maturation of DCs, triggering their ability to activate T cell responses (3). Induction of tumor-specific $CD8^+$ T cells is an appealing therapeutic strategy because the generated CTLs mediate Ag-specific killing of the targeted tumor via cell–cell contacts, as well as provide the host with long-lasting memory responses that may prevent cancer recurrence (5).

Liposomal vesicles can promote Ag delivery to the cytosol of APCs and subsequently enhance a CTL response, but not effectively. Different strategies based on liposomal vesicles were designed with the intention of streamlining these functions: examples include acidic pH-sensitive liposomes (Lp) (6, 7), cationic Lp (8, 9), and the inclusion of immunomodulators, such as TLR ligands (10, 11). Liposomal preparations including membranotropic peptides and bacteria pore-forming proteins (PFPs) also were investigated as novel cytosol-delivery systems for cross-priming cytotoxic $CD8^+$ T cells (12, 13). Particularly, encapsulation of listeriolysin O (LLO), a cholesterol (Cho)-dependent PFP from the Gram-positive intracellular pathogen *Listeria monocytogenes*, with Ags in pH-sensitive Lp significantly enhanced functional and protective CTL responses (14–16).

Sticholysins (Sts) I and II are PFPs from the Caribbean Sea anemone *Stichodactyla helianthus* belonging to a protein family called actinoporins (17). These cysteine-less and basic proteins of 20 kDa, exhibiting high structural similarity, are able to permeabilize cellular and model membranes by forming oligomeric pores of 2 nm diameter (18–20). Their permeabilizing activity is significantly enhanced by the presence of sphingomyelin (SM) (21, 22). The pore-forming activity of Sts makes these proteins attractive tools for cytosolic Ag delivery and enhancement of CTL immune responses.

In this study, we assessed the ability of Sts encapsulated into Lp with OVA to enhance an Ag-specific CTL response and their functionality in a murine tumor model. The liposomal formulation containing StII was able to induce a powerful OVA-specific CTL immune response, independent of $CD4^+$ T lymphocytes, under the experimental conditions assessed. Furthermore, a strong antitumor response in a preventive or therapeutic scenario was observed in animals immunized with these Lp and challenged with OVA-expressing E.G7-OVA tumor cells. This response was partially abrogated by depleting $CD8^+$ T cells.

Interestingly, by manipulating the structure of StI, its pore-forming activity and ability to stimulate CTL immune responses were decoupled. Moreover, StII induced the maturation of DCs in vitro, which may support its immunomodulatory properties.

Materials and Methods

Proteins, reagents, and tumor cells

StII (Swiss Protein Data Bank P07845) was purified from the sea anemone *S. helianthus* and characterized as described by Lanio et al. (18). Recombinant StI (rStI) and its mutant StI W111C were obtained according to the procedures described by Pazos et al. (23) and Pentón et al. (24), respectively. The protein concentration was determined using absorption coefficients of 1.87, 2.13, and 1.65 ml/mg/cm at 280 nm for StII, rStI, and StI W111C, respectively (18, 24), and their cytolytic activities were monitored by hemolysis assay. These proteins were stored at −20°C until use. The reagent bis(maleimido)hexane (BMH) was purchased from Pierce (Rockford, IL). Chicken OVA grade V, polyinosinic-polycytidylic acid (PIC), fluorophore carboxyfluorescein (CF), LPS from *Escherichia coli*, and polymyxin B (pmxB) were obtained from Sigma-Aldrich (St. Louis, MO). Recombinant murine GM-CSF (rmGM-CSF) was purchased from PeproTech (Rocky Hill, NJ). CFSE was acquired from Invitrogen (Paisley, U.K.). The immunodominant $OVA_{257–264}$ peptide (SIINFEKL) (synthesized by the Center for Genetic Engineering and Biotechnology, Havana, Cuba) was dissolved in PBS (Na_2HPO_4 9.6 mM, NaCl 137 mM, KCl 2.7 mM, KH_2PO_4 1.47 mM [pH 7.4]) and stored at −20°C until use. Mouse IgG fraction anti-OVA antiserum and rabbit IgG fraction anti-StII antiserum were obtained and purified by the Immunology Laboratory, Faculty of Biology, University of Havana. For in vivo $CD4^+$ T and $CD8^+$ T cell depletion, mAbs were isolated by protein precipitation [$(NH_4)_2SO_4$] and dialysis of supernatants from GK1.5 (American Type Culture Collection, Manassas, VA) and YTS 169 (European Collection of Cell Cultures, Wiltshire, U.K.) hybridomas, respectively. Egg yolk phosphatidylcholine (PC), bovine brain SM, dipalmitoyl phosphatidylcholine (DPPC), and Cho were purchased from Avanti Polar Lipids (Alabaster, AL).

The tumor cell line E.G7-OVA, a subclone of EL4 (a C57BL/6-derived thymoma) stably transfected with the cDNA of OVA, pAc–neo–OVA (25), was kindly provided by Dr. V. Bronte (Istituto Oncologico Veneto, IRCCS, Padua, Italy). Cell lines were cultured in DMEM-F12 (Life Technologies, Waltham, MA) supplemented with 10% FCS (Life Technologies), 2 mM L-glutamine, 1 mM sodium pyruvate, penicillin (100 U/ml), and streptomycin (100 μg/ml) (Life Technologies, Grand Island, NY). Prior to mice challenge, cells were washed with DMEM-F12 to remove FCS.

Production of irreversible inactivated dimeric variant from the mutant StI W111C

An irreversibly inactive dimer of the mutant StI W111C ($_{irrev}$StI W111C) was obtained by cross-linking the monomeric variant of StI W111C with the homo-bifunctional reagent BMH. First, StI W111C was reduced by incubation with 0.1 M 2-ME for 30 min at 25°C, followed by filtration in a PD-10 column (GE Healthcare, Uppsala, Sweden) equilibrated with PBS containing 5 mM EDTA to eliminate 2-ME. BMH dissolved in DMSO (Sigma-Aldrich) was immediately added to StI W111C at a 2:1 protein/BMH molar ratio, and the

mixtures were incubated for 2 h at 4°C with constant stirring. $_{irrev}$StI W111C was purified using a Superdex 75 HR 10/30 column (Amersham Biosciences, Uppsala, Sweden) by fast protein liquid chromatography (Pharmacia LKB, Uppsala, Sweden) with PBS at a lineal flow of 0.382 cm/min after previous incubation with 0.1 M 2-ME (reducing agent). SDS-PAGE (26), under reducing conditions, was used to verify production of the irreversible dimer and its purity. StI W111C spontaneously forms a reversibly inactive dimer of the mutant StI W111C stabilized by a disulfide bridge (24) ($_{rev}$StI W111C).

Entrapment of OVA and Sts in Lp: characterization of vesicles

The procedure rendering dehydration–rehydration vesicles (DRVs) (27) was used to obtain multilamellar Lp encapsulating OVA with one of the following variants of Sts: StII, rStI, $_{rev}$StI W111C, or $_{irrev}$StI W111C (hereafter, the slash notation used with Lp indicates encapsulating). In brief, small unilamellar vesicles composed of DPPC (16 μmol) and an equimolar quantity of Cho were prepared by ultrasonication using a Sonics Vibra-Cell ultrasonic processor (Sonics & Materials, Newtown, CT) by alternating cycles of 30 s of sonication and rest. Immediately, small unilamellar vesicles were mixed with 80 μg of OVA and 10 μg of Sts. After freezing at −70°C, the mixture of Lp and proteins was lyophilized in an Edwards freeze dryer (Bristol, U.K.) for 24 h. The rehydration step was carried out by adding 50 μl of distilled water per 16 μmol phospholipids and incubating for 30 min at 45°C. Nonentrapped components were removed by washing twice with PBS and centrifugation at 16,000 × g for 15 min in a microcentrifuge Eppendorf 5415C (Sigma-Aldrich). Pellets were finally resuspended in the appropriate volume of PBS. Similar liposomal preparations were prepared in the absence of PFP (Lp/OVA). To estimate encapsulation efficiency and retention capacity of vesicles, proteins were mixed with their corresponding labeled proteins that were previously iodinated by the chloramine T method (28). Lp/[^{125}I]OVA, Lp/[^{125}I]OVA/Sts, and Lp/OVA/[^{125}I]Sts formulations were prepared. After centrifugation, the encapsulation percentage was calculated from radioactivity measurements (cpm) of total supernatant (TSN) and the final pellet (FP), as follows: encapsulation (%) = [FP cpm/(TSN cpm + FP cpm)] × 100. Liposomal formulations were kept at 4°C dissolved in PBS, and small aliquots were taken at different times to measure the total radioactivity (T) and the supernatant radioactivity after centrifugation (SN). Retention percentage was calculated as (T cpm 2 SN cpm) × 100/T cpm. Liposomal preparations were used immediately after reconstitution in all experiments.

To determine the presence of OVA or StII at the liposomal surface, Lp/OVA, Lp/StII, and Lp/OVA/StII preparations (0.962 μmol lipids/ml) were exposed to mouse anti-OVA (20 μg/ml) or rabbit anti-StII (10 μg/ml) polyclonal Ab. After a 1-h incubation at 37°C with the respective antisera, samples were washed three times with PBS and mixed with secondary anti-mouse IgG or anti-rabbit IgG Abs conjugated to FITC, diluted 1:32 and 1:200 in PBS, respectively, for 15 min at 4°C. Empty DRVs used as negative controls were subjected to similar treatment. Positive-fluorescence vesicles were detected by flow cytometry (Becton Dickinson, San Jose, CA).

The average size and polydispersity of Lp containing proteins were measured at 25°C by photon correlation spectroscopy in a ZetaPALS Potential Analyzer (Brookhaven

Instruments, Holtsville, NY). Samples were diluted (1:600) in filtered PBS to achieve optimal vesicle concentration.

Hemolytic activity assays

The hemolytic activity of Sts was assessed, as previously described (29), using a microplate reader (Multiskan EX; Labsystems, Helsinki, Finland). Human RBCs were resuspended in TBS (145 mM NaCl, 10 mM Tris-HCl [pH 7.4]), and the concentration of the cell suspension was adjusted with TBS to an apparent absorbance of 0.1 at 650 nm. Proteins were serially diluted 2-fold in saline TBS using flat-bottom 96-well microplates, and human RBCs were added to each well (200 µl final volume). Hemolytic activity determination of $_{rev}$StI W111C or $_{irrev}$StI W111C variants was carried out in the presence or absence of 0.1 M 2-ME.

Permeabilization assays

The permeabilizing activity of StII was assessed by analyzing CF leakage from large unilamellar vesicles (LUVs) comprising DPPC:Cho or PC:SM (1:1 molar ratio) in TBS, as described by Tejuca et al. (21). Phospholipid concentration was determined as previously described (30), and Cho concentration was determined using a commercial kit (cat. no. 1.14830.0001; Merck, Darmstadt, Germany). A FLUOstar OPTIMA microplate reader (BMG Labtech, Ortenberg, Germany) was used to measure fluorescence (λ_{exc} = 490 nm and λ_{em} = 520 nm). Each well of the microplate (SPL-Life Sciences, Seoul, South Korea) was filled with 200 µl of TBS plus 0.2 µM LUV. StII was added at final concentrations of 2.5–1400 nM. The fraction of vesicles with at least one pore (f) was calculated as: $f = (F_f - F_0)/(F_{max} - F_0)$, where F_0 and F_f represent the fluorescence values before and after adding PFP, respectively, and F_{max} is the fluorescence measured in the presence of 0.1% Triton X-100 (Merck).

Mice and immunization schedule

Female C57BL/6 mice (H-2^b) were obtained from the National Center for Laboratory Animals Production (Havana, Cuba). CD45.2^+ OT-1 (CD8^+ T cell TCR-transgenic mice expressing the TCR recognizing SIINFEKL in H2-K^b) and CD45.1^+ Ly5-congenic mice on the C57BL/6 background were purchased from the Jackson Laboratory (Bar Harbor, ME). Mice were kept in specific pathogen–free conditions at the Center of Molecular Immunology (CIM) animal facilities and were used at 6–8 wk of age. All procedures were carried out in compliance with the protocols approved by the CIM Institutional Committee for the Care and Use of Laboratory Animals (0017/2008).

Immunizations were performed s.c. or i.m., in the inferior right limb, by delivering 0.2 or 0.1 ml of liposomal preparation, respectively, per mouse. Two injections of Lp/OVA or Lp/OVA/Sts were given at a 12-d interval. Doses of each component per injection per mouse were as follows: DPPC: Cho 10 µmol, OVA 50 µg, and Sts (StII, rStI, $_{rev}$StI W111C, or $_{irrev}$StI W111C) 6.25 µg, unless otherwise specified. Where indicated, OVA adjuvanted in PIC (OVA/PIC) was used as positive control giving one dose of 1 mg of OVA plus 100 µg of PIC per mouse on day 0 and PIC only for the subsequent 2 d. For CTL assays with CD4^+ T cell depletion, two doses of OVA 50 µg plus 100 µg of PIC were injected into mice on days 0

and 12. To evaluate the humoral response, mice were immunized s.c. as described above, and they were bled at day 21 of the experiment.

Ag-specific CD8$^+$ T cell expansion and characterization of memory phenotype

Splenocytes from six OT-1 mice (CD45.2$^+$) were homogenized in PBS, and 25 × 10^6 cells, equivalent to 5.5 × 10^6 CD8$^+$ T cells (checked by FACS), were transferred i.v. into female Ly5 mice (CD45.1$^+$) at day 0. On day 2, Ly5 mice were immunized s.c. with Lp/OVA or Lp/OVA/StII (three mice per group) and boosted on day 14. Mice injected with PBS were used as control. Seven days after the second immunization, Ly5 mice were sacrificed, and the draining inguinal lymph node (LN) closest to the inoculation site was isolated. OVA-specific CD8$^+$ T cells from single-cell LN suspensions were identified by flow cytometry by staining of CD45.2 and CD8. For the memory phenotype assay, cells were also stained for CD62L and CD44.

Generation of bone marrow–derived DCs and maturation assays

Bone marrow–derived DCs (BMDCs) were generated as described elsewhere (31). Briefly, bone marrow cells were harvested from femurs and tibias of female C57BL/6 mice, and single-cell suspensions were cultured at a density of 2 × 10^6 cells in Petri dishes containing 10 ml of complete RPMI 1640 supplemented with 200 U/ml (20 ng/ml) rmGM-CSF. An additional 5 ml of complete RPMI 1640 containing 20 ng/ml rmGM-CSF was added on days 3 and 5 after culture. Cells were collected from each dish and counted on day 6. BMDCs (1 × 10^6 cells per milliliter) in six-well plates were pulsed with stimuli for 3 h followed by 18 h of incubation with 10% FCS [note that StII is inactivated in the presence of serum (32)]. Subsequently, BMDCs were analyzed by flow cytometry. Stimuli consisted of StII and LPS as positive control (both at 1 μg/ml), as well as StII and LPS mixed with pmxB (10 μg/ml) or StII that was purified previously using Detoxi-Gel Endotoxin Removing Gel column prepacked (Thermo Fisher Scientific, Waltham, MA). The StII purity was ~99% and contained <20 EU/mg protein.

Flow cytometry analysis

Cells were stained with specific Abs using conventional protocols. Lymphocyte characterization was performed with the following specific anti-mouse mAbs: CD8/allophycocyanin, CD8/PE, CD4/FITC, CD3/PECy5, CD62L/FITC, CD45.2/PE, and CD44/PECy5 (all from eBioscience, San Diego, CA). Cells were acquired using FACScan (BD Biosciences, San Jose, CA) and Gallios (Beckman Coulter, Miami, FL) flow cytometers and analyzed with FlowJo 7.6.1 (TreeStar) software. In BMDC maturation assays, cells were stained with anti-mouse CD11c/PE, CD86/allophycocyanin, CD40/FITC, CD80/FITC, CD80/PE (all from eBio-science), anti-mouse CD11c/allophycocyanin, and CD40/PE Texas Red (both from BD Biosciences). A LIVE/DEAD Fixable Aqua Dead Cell Stain Kit (Invitrogen) was used to exclude dead cells. Stained cells were detected using a FACSCalibur (BD Biosciences) flow cytometer and analyzed with FlowJo 7.6.1 software. Doublets were excluded from total acquired cells by the analysis of forward scatter (FSC)-area versus FSC-high parameters.

Ag-specific CTL assay in vivo

Total splenocytes of naive C57BL/6 mice were pulsed or not (internal control) with 1 μM SIINFEKL for 60 min at 37°C and 5% CO_2. Peptide-pulsed target cells were washed extensively to remove free peptide. Subsequently, target cells were labeled with the fluorescent dye CFSE ($CFSE^{bright}$; 5 μM) for 5 min at 37°C and washed twice. Unpulsed cells were simultaneously labeled with the fluorescent dye ($CFSE^{dull}$; 0.33 μM). Cells were mixed at a 1:1 ratio, and 60×10^6 cells were injected i.v. into immunized mice on day 20. Sixteen hours later, mice were sacrificed, the inguinal LN closest to the site of immunization was removed, and the total events corresponding to both fluorescent intensities ($CFSE^{dull}$ and $CFSE^{bright}$) were determined by flow cytometry. The percentage lysis for each mouse was calculated as follows: percentage lysis = $100 - (CFSE^{bright}/CFSE^{dull})_{vaccinated} \times 100 \times (CFSE^{dull}/CFSE^{bright})_{PBS}$. Experimental groups (three mice per group) received s.c. PBS, OVA/PIC, Lp/OVA, or Lp/OVA/Sts, as indicated above. In some experiments, depletion of $CD4^+$ T cells was carried out by i.p. injection of a specific mAb (anti-CD4, 1 mg) for 4 d, starting 1 d before the first immunization. An immunized control group received PBS instead of anti-CD4 mAb. Depletion was checked by flow cytometry.

Tumor challenge assays

Mice (6–10 per group) were immunized s.c. or i.m. with PBS (control), Lp/OVA, or Lp/OVA/StII, as described above. In some experiments, a group of mice received half a dose of OVA, as well as half of the corresponding total lipids and StII. On day 7 postboost, animals were challenged by s.c. injection of 3×10^5 E.G7-OVA cells in 200 μl of DMEM-F12 into the right flank. Tumor growth was monitored every 2–3 d by measuring the two largest perpendicular diameters with a caliper, and the tumor volume (tV) was calculated ($tV = \pi/6 \times \text{length} \times \text{width}^2$). Mice with one diameter ≥ 2.0 cm were euthanized following the guidelines of the CIM Institutional Committee for the Care and Use of Laboratory Animals (0017/2008), and survival was scored as the percentage of surviving animals. The percentage of mice without tumor was also recorded. An antitumor assay was also carried out using a specific mAb to deplete the $CD8^+$ T cell population (anti-CD8). In this case, 1 mg of this mAb was injected i.p. into immunized mice 1 d before tumor implantation. This dose was shown to deplete >95% of $CD8^+$ T cells (33). An immunized control group received PBS instead of anti-CD8 mAb. The immunotherapeutic effect of vaccination was also assessed by challenging mice with tumor at day 0 and 3 d after they were immunized with three doses of the Lp formulations at 1-wk intervals.

Analysis of OVA- and StII-specific Ab titers

OVA- and StII-specific IgG titers in serum were measured by ELISA using OVA or StII (10 μg/ml)-coated plates (Greiner Bio-One, Frickenhausen, Germany). Mice sera diluted 1:100 were added to wells in triplicate and further serial dilutions were performed. Specific Abs were detected with alkaline phosphatase–conjugated goat anti-mouse total IgG (Sigma-Aldrich) or biotinylated goat anti-mouse IgG1 or IgG2c Abs (AbD Serotec, Oxford, U.K.), followed by alkaline phosphatase–conjugated streptavidin (Sigma-Aldrich) in the two last determinations. The absorbance was read at 405 nm using *p*-nitrophenyl phosphate (Sigma-Aldrich) as substrate.

Statistical analysis

The normal distribution of data was analyzed by the Kolmogorov–Smirnov test, followed by the Bartlett or Levene test to check variance homogeneity. The means from two independent samples were compared using the unpaired *t* test (two-tailed) or Mann–Whitney *U* test. Statistically significant differences between means from three or more unmatched groups were determined using one-way ANOVA or the Kruskal–Wallis test. The Tukey, Dunnett T3, or Dunn test was used for comparison of multiple means. Survival and tumor-free mice percentages were analyzed using the Kaplan–Meier estimation, followed by the log-rank test. Statistical analyses were conducted using GraphPad Prism 5, version 5.01 (GraphPad) software, with the exception of the Dunnett T3, Kaplan–Meier, and log-rank tests, which were performed using the statistical software package SPSS version 16.0. $p < 0.05$ was considered statistically significant.

Results

Lp comprising DPPC:Cho are suitable for encapsulating the PFP StII

Sts readily bind to model membrane systems, such as lipidic monolayers, micelles, and lipid vesicles (21, 22, 34–36). These PFPs exhibit high irreversible binding affinity for SM-containing membranes, and the presence of this lipid significantly enhances their pore-forming ability (21, 22). Considering the lipid requirement for the permeabilizing activity of Sts, we evaluated the ability of StII, the most active of Sts (29), to generate pores in DPPC:Cho vesicles by measuring CF efflux from LUVs upon PFP addition (Fig. 1). As expected, the fraction of the PC:SM vesicles permeabilized at the steady-state (f_{max}, fluorescence achieved at 30 min) increased as a function of StII concentration, exhibiting activity in the nanomolar concentration range (22, 29). In contrast, the permeabilization of DPPC:Cho vesicles by StII was nearly negligible, even at protein/lipid ratios considerable superior to those used in the DRVs formulation (see *Materials and Methods*) (Fig. 1). Taken together, these results show that DPPC:Cho in a 1:1 molar ratio is an acceptable lipid composition to achieve the encapsulation of Sts together with OVA as a model Ag.

The DPPC:Cho DRVs exhibited a relative high efficacy of encapsulation for StII (52 ± 8%), retaining >70% of this protein after 28 d of storage in suspension at 4°C (Supplemental Fig. 1). In the formulations containing or not containing StII, OVA was encapsulated with similar efficacy (48 ± 7% and 57 ± 10%, respectively) and was similar to that observed for StII ($p > 0.05$). The retention capacity of DPPC:Cho Lp for OVA (>40%) also was independent of the presence of StII, even after a long incubation period (28 d) at 4°C (Supplemental Fig. 1). The similarity in the OVA encapsulation and retention in Lp in the presence or absence of StII indicates that this protein does not affect Ag entrapment in these vesicles. Although StII was retained inside Lp more efficiently than OVA over the storage time, it is interesting to note that both proteins had a similarly high retention percentage at the first week of incubation (>80%, Supplemental Fig. 1). The higher retention for StII could be related to the ability of this PFP, although very limited, to bind but not destabilize lipid membranes containing PC and Cho (22, 37).

We also evaluated the presence of OVA and StII on the liposomal surface by flow cytometry using specific polyclonal Abs against each protein. Dot plot graphs representative of each liposomal sample illustrate the proportion of vesicles carrying at least one molecule of StII and OVA at the liposomal surface (Fig. 2A). Several liposomal formulations were analyzed, and the percentage of the vesicles positive to labeling for each protein on the surface are shown in Fig. 2B and 2C. The fraction of Lp/OVA vesicles carrying OVA on their surface was similar to that of Lp/OVA/StII vesicles ($p = 0.471$), and comparable behavior was observed for Lp/StII and Lp/OVA/StII vesicles ($p = 0.459$) with respect to StII. The results indicate that OVA and StII are exposed in an equivalent proportion of vesicles (~25%) without influencing each other. These results are in agreement with the efficiency of encapsulation and retention for both proteins (Supplemental Fig. 1) and suggest that StII and OVA do not seem to compete with each other during vesicle preparation.

Furthermore, we measured the size and polydispersity of DRVs carrying OVA, with or without StII, and observed relatively high sizes for both particles (1.6 ± 0.07 and 2.2 ± 0.04 μm for Lp/OVA and Lp/OVA/StII, respectively), in agreement with the previously reported size for this type of Lp (diameters ranging from 0.1 to 2 μm) (38, 39). The entrapment of OVA alone or together with StII into the Lp increased the particle sizes in comparison with empty Lp (data not shown). Additionally, Lp/OVA and Lp/OVA/StII preparations also showed significant differences in particle size (unpaired *t* test, $p = 0.0016$), which could result from the necessary changes in vesicle volume to better accommodate the entrapped solutes. In accordance with the observed sizes, vesicles also exhibited relatively high polydispersity indexes, albeit those with larger size showed smaller indexes (Lp/OVA/StII 0.24 ± 0.03 and Lp/OVA 0.4 ± 0.02, $p = 0.0056$, unpaired *t* test). The high and low isoelectric point of StII (pI > 9.0) (18) and OVA (pI = 4.5) (40), respectively, could favor the electrostatic interaction among these proteins inside Lp and contribute to the compactness and, hence, homogeneity of the vesicles. Lanio et al. (35) explained the interaction of Sts with anionic surfactants by their high isoelectric points and a preferential electrostatic binding at the working pH (7.4). A similar event could be occurring in this case.

DPPC:Cho Lp containing StII expand OVA-specific CD8$^+$ T cells with memory phenotype and enhance OVA-specific CTL responses in vivo independent of CD4$^+$ T cell help

To evaluate the ability of the Lp/OVA/StII formulation to activate CD8$^+$ T lymphocytes in vivo, we first studied the effect of Lp/OVA/StII versus Lp/OVA on the population of OVA-specific CD8$^+$ T cells in the draining LN. For this purpose, we adoptively transferred CD8$^+$ T lymphocytes from OT-1 mice (CD45.2$^+$) into Ly5 mice (CD45.1$^+$). Mice immunized with Lp/OVA/StII showed a significant increase in the percentage of OVA-specific CD8$^+$ CD45.2$^+$ T cells in relation to those receiving PBS ($p = 0.0001$) or Lp/OVA ($p = 0.0014$) (Fig. 3A, 3B). Animals treated only with PBS exhibited the lowest percentage of these cells (Fig. 3B), whereas immunization with Lp/OVA did not result in a significant difference in the amount of OVA-specific CD8$^+$ T lymphocytes compared with PBS ($p = 0.08$). This result shows that Lp/OVA/StII promotes a remarkable expansion of Ag-specific CD8$^+$ T cells compared with Lp/OVA, probably as a result of an enhanced StII-mediated Ag cross-presentation by APCs to these cells. Surprisingly, the percentage of the predominantly OVA-nonspecific CD45.2$^+$ CD8$^-$ cell population increased noticeably in response to both

liposomal formulations (Fig. 3A), which suggests that these Lp could be stimulating other leukocytes, even in an Ag-independent manner. A further characterization of the OVA-specific $CD8^+$ T cell population was performed by evaluating the expression of memory markers on their surface. Although both liposomal preparations elicited OVA-specific $CD8^+$ T lymphocytes with memory phenotype ($CD44^{high}$ $CD62L^+$), the highest proportion was associated with Lp/OVA/StII immunization, with a mean that was significantly superior to that of PBS ($p = 0.0014$) or Lp/OVA ($p = 0.011$) (Fig. 3C, 3D). In contrast, mice treated with Lp/OVA showed a higher frequency of memory $CD8^+$ T cells than did those that received PBS ($p = 0.03$). Collectively, these results illustrate that Lp/OVA/StII and Lp/OVA formulations differ with regard to the frequency of Ag-specific $CD8^+$ T lymphocytes and precursors with memory phenotype elicited by them.

The above-described results support the hypothesis that StII coencapsulated with an Ag into DPPC:Cho Lp could favor the Ag presentation in the MHC class I by APCs in vivo, probably enhancing an Ag-specific CTL response. To validate this hypothesis, we assessed OVA-specific CTL responses induced in vivo by Lp/OVA/StII (Fig. 4A, 4B). All experimental treatments were effective, because induced target cell lysis percentages were significantly superior to PBS ($p < 0.05$). However, immunization with Lp/OVA/StII produced an OVA-specific lysis significantly larger than Lp/OVA ($p = 0.005$) and OVA/PIC ($p = 0.022$) (positive control), being in some animals higher than 95%. In contrast, Lp/OVA and OVA/PIC showed similar percentages of target cell lysis ($p = 0.803$), probably supported by the small frequency of OVA-specific $CD8^+$ T cells with memory phenotype induced by Lp/OVA. These results demonstrate that StII coencapsulated with the Ag into Lp significantly enhances an Ag-specific CTL response. In agreement with the expansion of the OVA-specific $CD8^+$ T cells induced by Lp/OVA/StII formulation in the preceding experiment (Fig. 3B), these results support a role for StII in Ag cross-presentation.

The dependence on help mediated by $CD4^+$ T cells for priming of Ag-specific $CD8^+$ CTL responses has been very well documented (41–43). However, a high level of inflammation accompanying Ag recognition (e.g., viral or bacterial infection), as well as immunization with some adjuvants (PIC, very small size proteoliposome [VSSP]), can induce primary CTL responses independent of $CD4^+$ Th cells (44–46). To evaluate whether the CTL response induced by the Lp/OVA/StII adjuvant system depends on $CD4^+$ T cell help, we depleted $CD4^+$ T cells by systemic treatment with an anti-CD4 mAb. Mice injected with PBS were used as a control group. The effectiveness of depletion was checked by analyzing the residual presence of $CD4^+$ T cells after 24 h (19% for PBS group versus 1% for treated animals) (Fig. 4C). Because a partial recovery was detected at day 4 (8%), we treated animals with the mAb at 4-d intervals during the experiment. Groups immunized with Lp/OVA/StII exhibited similar lysis percentages whether or not $CD4^+$ T cells were depleted (66.8 and 74.7%, respectively, $p = 0.559$) (Fig. 4D). This behavior was similar to that observed in the group receiving OVA/PIC ($p = 0.840$), which was used as control based on the previous demonstration that induction of CTLs by PIC was independent of $CD4^+$ T cell help (45). This experiment demonstrates that, even in the absence of $CD4^+$ T cells, immunization with Lp/OVA/StII is able to induce high levels of target cell lysis (~70%).

OVA-specific Ab titer was measured from immunized mice serum at the same time as the CTL assays to investigate whether the inclusion of StII in DPPC:Cho Lp is also able to provide nonescaped OVA to the MHC class II pathway for priming of humoral immunity. At 21 d after the first immunization, liposomal OVA induced significantly higher levels ($p < 0.05$) of OVA-specific total IgG, IgG1 (Th2-type), and IgG2c (Th1-type) Ab responses, regardless of the presence of StII inside Lp, in comparison with those observed with the soluble OVA (PBS+OVA) as control group (Supplemental Fig. 2A – C). This result reveals that the incorporation of StII into Lp does not cause any additional effect on the MHC class II OVA-presenting pathway, which is just enhanced by the very well documented adjuvant capacity of Lp (47, 48). Additionally, all of the above-described results indicate that the liposomal Ag combined with StII continues its transit by both Ag-presenting pathways and confirm the ability of Lp to elicit a Th1/Th2 mixed-Ab response (49). Previous results obtained by our group demonstrated that DPPC: Cho (1:1) Lp encapsulating human epidermal growth factor are able to modulate the anti–human epidermal growth factor Ab response in mice to a mixed Th1/Th2 response, but they favored a Th1 pattern (50). The ability of Lp/OVA/StII to induce a Th1/Th2 mixed pattern could be desirable for a candidate vaccine that is addressed not only to intracellular targets (51).

The anti-StII humoral immune response was also analyzed under the experimental conditions described. The total-IgG Ab response elicited by DPPC:Cho Lp containing StII and OVA was compared with the response generated by StII mixed with OVA in PBS at day 21. As shown in Supplemental Fig. 2D, mice immunized with StII in solution or encapsulated into DPPC:Cho Lp presented equivalent titers of anti-StII IgG Abs. These results indicate that StII is an immunogenic protein, but in lower extension than OVA, and it does not interfere in the OVA-specific cellular and humoral responses. In addition, StII immunogenicity is not increased by Lp under the experimental conditions described.

Immunization with DPPC:Cho Lp encapsulating StII improves an antitumoral immunity partially dependent on $CD8^+$ T cells

DPPC:Cho Lp containing StII showed to be a promising vaccine candidate to generate cytotoxic $CD8^+$ T cells; however, it was important to evaluate whether that enhanced CTL response was effective in conferring protective immunity. E.G7-OVA thymoma, a murine tumor model expressing OVA, was used to evaluate the ability of Lp/OVA/StII to protect against tumor cells.

First, we explored two routes and doses of Lp/OVA/StII administration in a tumor-protection assay. Two groups of mice received 50 μg of OVA i.m. or s.c., and a third group was treated with 25 μg of OVA s.c. Seven days after the second immunization, animals were challenged with E.G7-OVA cells. All immunization strategies were effective in developing an antitumoral response compared with the PBS group (negative control), which rapidly developed tumors by days 9–10 (Supplemental Fig. 3). Although an apparently higher efficacy ($p = 0.012$, day 22) in terms of tumor progression was observed with the s.c. route and the higher dose of OVA (50 μg), similar results ($p > 0.05$) for all tested regimens were clearly evidenced for tumor-free mice and survival percentages. These data demonstrated that the Lp/OVA/StII formulation is able to induce an obvious protection against tumor, even

at the half doses used in the CTL assays. It is also relevant that this formulation provided success via the two parenteral routes of immunization described. Therefore, we used both indistinct routes of immunization with the highest doses assessed in the following antitumor assays.

Because Lp/OVA and Lp/OVA/StII showed the ability to stimulate a CTL response, but at different magnitudes (Fig. 4A, 4B), their efficacy in prophylactic antitumor activity was also compared. With this purpose in mind, mice were immunized i.m. with Lp/OVA/StII or Lp/OVA before being challenged with the tumor cells. At day 18, both groups immunized with Lp had statistically similar tV averages ($p = 0.16$), but they were remarkably inferior ($p < 0.001$) to the PBS group (Fig. 5A). However, significant differences between these two groups were observed with regard to other parameters measured. The tumor appeared in the Lp/OVA/StII group at day 21 after tumor challenge, whereas it appeared at day 11 in the Lp/OVA group (Fig. 5B). Importantly, significantly higher percentages of Lp/OVA/StII-immunized mice remained tumor-free ($p = 0.022$, Fig. 5B) or survived ($p = 0.016$, Fig. 5C) compared with Lp/OVA-immunized mice. In summary, immunization with Lp/OVA/StII was able to enhance an Ag-dependent antitumor immunity compared with Lp/OVA, which might be strongly related to the behavior of both liposomal formulations observed in the CTL response.

The role of effector $CD8^+$ T lymphocytes in the antitumoral response was determined by depleting these cells in experimental mice with an anti-CD8 mAb. Mice immunized s.c. with Lp/OVA/StII and depleted of $CD8^+$ T cells experienced a significant reduction in the retardation of tumor growth ($p < 0.01$), as well as in the percentages of tumor-free mice ($p = 0.001$) and survival ($p = 0.001$) (Fig. 5D – F), in relation to those immunized with Lp/OVA/StII but receiving PBS instead of anti-CD8 mAb. Interestingly, total abrogation of antitumoral activity was not observed upon $CD8^+$ T cell–depletion treatment ($p < 0.01$ for all parameters measured), indicating the putative presence of other effector cells. This result confirms that $CD8^+$ T lymphocytes stimulated by immunization with Lp/OVA/StII notably contribute to the antitumoral response but that other types of cell populations of the immune system also could be influencing this response.

The antitumor effects of Lp/OVA/StII and Lp/OVA were also compared in a therapeutic setting; animals were immunized s.c. three times 3 d after challenge with tumor cells. As shown in Fig. 6, immunization with Lp/OVA did not induce any significant effect compared with PBS in tumor bearing-mice ($p > 0.05$). In contrast, animals immunized with Lp/OVA/StII exhibited a reduction in tV ($p < 0.05$) and an increase in the percentage of tumor-free mice ($p = 0.016$) in relation to the control group, but there was no statistically significant difference compared with the group treated with Lp/OVA, at least under the experimental conditions assessed. However, changes in the immunization schedule, for example, could magnify the difference between both groups. Nevertheless, we could take as fact that StII added to DPPC:Cho Lp improves antitumor activity in preventive and therapeutic scenarios, which is important in the design of different vaccination strategies.

Stimulation of the OVA-specific CTL response by DPPC:Cho Lp encapsulating StII does not depend only on its pore-forming ability

StII and StI exhibit high homology at the sequence and three-dimensional structural levels (18, 19, 52). Mutants containing a cysteine residue in relevant functional regions of rStI were designed and obtained, exhibiting a different ability to form dimeric structures stabilized by disulfide bridges (24, 53). Among them, StI W111C, with a cysteine residue at the membrane-binding region, displayed a high propensity to form a reversibly inactive dimer ($_{rev}$StI W111C) as a result of its inability to bind to membranes (24, 54). This molecular entity was a nice tool to produce an irreversibly inactive dimer by StI W111C conjugation, using the chemical reagent BMH ($_{irrev}$StI W111C, Supplemental Fig. 4A). The conjugation yield for the irreversible entity was ~30% (Supplemental Fig. 4B, lane 3), with a lower amount of the reversible form (~14% of the total amount of protein in the reaction). The purification of $_{irrev}$StI W111C previously incubated under reducing conditions allowed separation of this inactive dimeric form from the other molecular entities present; its purity was corroborated by SDS-PAGE (Supplemental Fig. 4C, 4D). $_{irrev}$StI W111C constituted ~94% of the total protein (Supplemental Fig. 4D, lane 5), whereas only a small amount of the reversible dimer was present (<6%). As expected, $_{irrev}$StI W111C did not exhibit pore-forming ability, as assessed by a hemolytic assay, even in a reducing environment. Under these conditions, the presence of reversible dimer was almost negligible (1.5%), at least in terms of its functionality (data not shown).

The coencapsulation efficiency of rStI, $_{rev}$StI W111C, and $_{irrev}$StI W111C with OVA into DPPC:Cho Lp was equivalent to that observed for StII in Lp/OVA/StII (~57%). In addition, the efficacy of OVA encapsulation was independent of the presence of Sts and was similar to the values reported above.

Surprisingly, in the CTL assay, mice immunized with Lp/OVA/$_{irrev}$StI W111C showed an Ag-specific lysis percentage that was equal to mice receiving Lp/OVA/rStI or Lp/OVA/$_{rev}$StI W111C (Fig. 7). The dashed line indicates the average value of target cell lysis (%) in animals immunized with Lp/OVA/StII (Fig. 4B) and shows that all experimental groups treated with Lp containing any of the St variants exhibited similar efficacy to this formulation. This result also indicates that rStI retains the capability of StII to stimulate a strong OVA-specific CTL response. Additionally, $_{rev}$StI W111C coencapsulated into Lp with OVA seems to behave as a PFP, which is activated by sulfhydryl groups and is able to enhance the activation of $CD8^+$ T cells. As mentioned previously, groups treated with OVA/PIC showed lower percentages of target cell lysis. From the results observed with Lp/OVA/$_{irrev}$StI W111C, we hypothesize that the pore-forming activity of Sts is not crucial for enhancement of Ag-specific CTL immune responses by DPPC:Cho Lp. Instead of the pore formation in the endosomal membranes, any other mechanism conditioned by the Sts structure is more relevant in the CTL response.

The PFP StII induces DC maturation

As has been very well established, activation of naive $CD8^+$ T cells occurs via stimuli-activated APCs. With the purpose of elucidating whether the maturation of DCs by StII is a mechanism involved in the immunomodulatory properties of Sts, we investigated whether

LPS-free StII could induce this process. The experiment was corroborated using LPS as a positive control in the presence or absence of pmxB, a cationic cyclic lipopeptide that binds the lipid A moiety of LPS and blocks its biological effects (55). Fig. 8 shows that $CD11c^+$ cells (DCs) express higher levels of the costimulatory molecules CD86, CD40, and CD80 when stimulated with StII compared with nonstimulated cells. The increase in these cellular markers elicited by StII plus pmxB was higher compared with DCs treated with pmxB (negative control) (Fig. 8A, 8B). In contrast, DCs incubated with LPS mixed with pmxB exhibited values that were similar to the negative control. This result reveals a DC maturation effect that is induced by StII, even in the presence of pmxB. The immunomodulatory property of StII was further confirmed using an endotoxin-free protein purified using a Detoxi-Gel Endotoxin Removing Gel column. After purification, StII still induced an increase in DCs expressing CD40 and CD80 surface molecules (Fig. 8C). Addition of pmxB to pure StII did not change the effect observed (data not shown). In summary, these results demonstrate that StII induces maturation of DCs in vitro and could suggest a contribution by this immunomodulatory effect to the immune response mediated by St Lp.

Discussion

The development of a vaccine strategy for eliciting functionally robust CTL responses depends primarily on the ability to efficiently introduce exogenous antigenic proteins into the MHC class I pathway of APCs. In this sense, there are interesting vaccine platforms based on several delivery strategies that direct Ags toward the APCs' cytosol (56). Bacterial PFPs, particularly LLO from *L. monocytogenes*, have been used to mediate Ag cytosolic delivery and improve CTL-mediated immune responses (13, 14). With regard to this, the potential use of PFPs from other non-bacterial sources as immunomodulators and exhibiting different structural and functional properties, such as tridimensional structures, nature of formed pores, and pH dependence and lipid requirement for the pore formation, among others, could be interesting and promising.

Our results demonstrate that noncationic and nonfusogenic lipids-containing Lp, but encapsulating a model Ag together with a PFP classified in the family of actinoporins, are able to induce a potent and functionally protective Ag-specific CTL response. We proved that this liposomal formulation favors Ag cross-presentation and functions as a potent vaccine adjuvant to initiate APC–T cell interactions and to stimulate $CD8^+$ T cell– mediated immune responses. Moreover, the evidence described in this article point out that the pore-forming activity of Sts is not essential for eliciting an Ag-specific CTL response.

The liposomal lipid composition based on DPPC/Cho, at a 1:1 molar ratio, was chosen to minimize membrane–Sts interactions and, as a consequence, the pore-forming ability of Sts. Because SM is considered a natural membrane acceptor for actinoporins (22, 57), its exclusion was essential. Based on previous reports (58, 59), lipid compositions generating lipid phase coexistence, which favors membrane insertion of actinoporins, were also avoided. The absence of permeabilization activity of StII in DPPC:Cho LUVs (Fig. 1) indicates the feasibility of encapsulating Sts into these Lp to perform in vivo assays. In fact, the relatively high and equivalent encapsulation efficacy of DPPC:Cho DRVs for all proteins

assessed (~50%) and their relatively elevated stability, at least in term of their retention capacity during the first 7 d of storage in suspension (Supplemental Fig. 1), confirms this statement. These results agree with those reported previously for DRVs that are characterized by a large internal volume with moderate to high encapsulation and retention efficiency (27, 60). Additionally, the low proportion of vesicles carrying at least one molecule of StII or OVA on their surface (Fig. 2) supports that most of these proteins are trapped inside the Lp. In summary, the DRVs procedure used to prepare DPPC:Cho Lp, rendering a highly organized membrane resulting from selected lipid composition (37, 61), indicates that it is possible to administer Lp/OVA/StII even a few days after its reconstitution because these vesicles remain essentially intact.

The large sizes of DRVs carrying OVA, and containing StII or not, could contribute to an avid uptake by phagocytic cells, specifically macrophages (62). However, macrophages do not show an Lp size-dependent pattern of uptake (63); thus, we could expect a similar degree of internalization for both liposomal formulations by these APCs. In addition, OVA-containing Lp, obtained as described in this article, do not differ from empty Lp in zeta potential, being around −25 mV (Y. Cruz-Leal and M.E. Lanio, unpublished observations). Similar results were reported by Nordly et al. (64) using cationic Lp carrying OVA adsorbed at their surface. In contrast, in this study, the molar ratio of StII and lipids in Lp/OVA/StII is notably lower than that used for OVA; therefore one might presuppose minimal or no influence of StII on the surface potential of Lp. Considering this, we believe that the difference in immunomodulatory properties observed between Lp/OVA and Lp/OVA/StII could be due to some property of StII, rather than advantageous physicochemical characteristics of Lp/OVA/StII in relation to Lp/OVA.

The ability of Lp/OVA/StII to enhance Ag presentation by MHC class I was studied by following stimulation of the $CD8^+$ T cell population in vivo. The expansion of OVA-specific $CD8^+$ T cells, observed in mice treated with such a liposomal formulation and not in those receiving Lp/OVA (Fig. 3B), demonstrated the requirement for StII inside Lp to induce, at least more efficiently, MHC class I–mediated Ag presentation. Consequently, the amount of $CD8^+$ T cells expressing $CD44^{high}$ and CD62L, as markers of memory T lymphocytes (65, 66), elicited by Lp/OVA/StII was higher than that observed with Lp/OVA (Fig. 3D). In addition, we presuppose that Lp/OVA/StII, as a result of the presence of StII, could also be causing a higher epitope density on APCs than Lp/OVA, which results in a higher number of $CD8^+$ memory T cells that is generated and persist in the host, according to Leignadier and Labrecque (67). This ability of Lp/OVA/StII could have relevance in future applications, because the development of vaccines capable of inducing long-lived memory $CD8^+$ T cells is desired to establish a stage of immune surveillance.

Because several pathways exist for loading antigenic peptides onto MHC class I molecules (56), we could only hypothesize about a probable internal mechanism followed by Lp/OVA/StII that explains its enhancement of MHC class I–mediated Ag presentation. Such a process that should necessarily involve the uptake of Lp by APCs and Lp destabilization in the endosomal compartment is probably followed by StII-mediated endosomal rupture, and the subsequent release of the vesicle content leading to Ag presentation by the MHC class I pathway, as was proposed for LLO-containing Lp (68, 69). Recent results obtained by our

group support the relevant role of Lp/OVA/StII in mediating Ag cross-presentation in vitro in comparison with Lp/OVA and suggest a main role for macrophages in this process (Y. Cruz-Leal, D. Grubaugha, C. Nogueira, I. Lopetegui, A. del Valle, F. Escalona, R. Laborde, C. Mesa, L. E. Fernández, M. Starnbach, D. Higgins, and M.E. Lanio, manuscript in preparation). Indeed, the function of macrophages in the stimulation of naive $CD8^+$ T cells and cross-presenting Ags in vivo also was demonstrated previously (70). The Ag-specific cross-presentation was further confirmed by the highest specific lysis of target cells induced with Lp/OVA/StII in the CTL assays in vivo (Fig. 4B). In fact, StII incorporated into Lp was able to enhance the OVA-specific CTL response, and this property was reproduced by the other isoform, StI obtained via recombination (Fig. 7). Altogether, the results from both assays ($CD8^+$ T cell expansion and in vivo CTL response) indicate that Sts-containing Lp induce a substantial proliferation of OVA-specific $CD8^+$ T lymphocytes that act as CTL precursors, provoking the notable CTL-mediated immune response in mice. A correlation between $CD8^+$ T cell expansion and the number of CTLs was documented (71).

$CD4^+$ Th cells have several important roles during the development and maintenance of CTL responses, including the enhancement of clonal expansion during priming (43). Interestingly, under the described experimental conditions, the OVA-specific CTL immune response enhanced by Lp/OVA/StII was independent of $CD4^+$ Th cells (Fig. 4D), as was similarly established for other adjuvants, such as PIC and VSSP (45, 46). It is known that infectious agents can provoke an Ag-specific CTL response, independent of $CD4^+$ Th cells, as a consequence of the induction of strong inflammatory stimuli in the primary response by potent TLR activation of APCs (72). This would explain the independence of the adjuvants PIC and VSSP with regard to $CD4^+$ T help. Nevertheless, it is noteworthy that Lp/OVA/StII induces an equivalent response but lacks conventional TLR ligands. However, for PIC, such independence was only observed in the primary response, because the MHC class II–restricted Th cell response was required to generate a memory CTL response (43). A recognized role for $CD4^+$ Th cells in generating functional and sustainable memory $CD8^+$ T cells also was established for inflammatory and noninflammatory agents (73). In contrast, $CD4^+$ T cells were not required for the generation of memory $CD8^+$ T cells in the case of immunization with Lp-coupled OVA-peptides mixed with CpG (74). Consequently, it would be necessary to investigate whether the OVA-specific and long-lasting memory CTL immune response enhanced by Lp/OVA/StII depends on the provision of an appropriate Th cell response. Even so, the apparent autonomy of specific $CD8^+$ T lymphocyte responses from Th cells could be pertinent to achieve a CTL response in immunocompromised individuals.

In agreement with the results obtained in the CTL assays in vivo, a significant protection was observed in mice immunized with Lp/OVA/StII and challenged with OVA-bearing tumor cells in terms of tV, tumor-free mice, and survival compared with groups treated with Lp/OVA or PBS, indicating that the Ag-specific CTL response was robust (Fig. 4B), as well as functional (Fig. 5A–C). A comparable correlation was obtained with a pH-sensitive liposomal preparation carrying LLO and OVA (14). Other similar approaches to induce antitumoral protection consist of Lp containing fusogenic proteins from virus (75) or membranotropic peptides (76). Nevertheless, in the present vaccine platform, neither fusogenic nor pH-sensitive Lp were used to carry a nonbacterial PFP. In addition, the

contribution of $CD8^+$ T lymphocytes to the antitumor activity induced by Lp/OVA/StII was demonstrated by its significant reduction in the absence of these cells (Fig. 5D–F). However, the antitumor protection was only partially abrogated with $CD8^+$ T cell depletion, suggesting that other immune cells take part in this process. This observation could be also correlated with expansion of the predominantly OVA-nonspecific $CD8^-$ cell population that was induced by Lp/OVA/StII at the draining LN (Fig. 3A). Both results suggest that this liposomal formulation, in addition to $CD8^+$ T cells, could be stimulating the expansion of other kind of leukocytes, Ag or non-Ag specific, that could contribute to the antitumor response. Clones of OVA-specific $CD4^+$ T cells are activated by Lp/OVA/StII immunization, as was confirmed by the anti-OVA Ab titers induced by these vesicles (Supplemental Fig. 2A – C). These cells probably collaborate with $CD8^+$ T cells in the antitumoral activity similar to that reported by Kim et al. (77) using Lp coencapsulating OVA and CpG. In addition, Lp/OVA/StII and Lp/OVA expanded the $CD8^-$ cell population; therefore, common features of these vesicles could be further modulating such cells. Cells from the innate immune system, such as NK and NKT cells, could be expanded by these vaccinations, as observed under different stimuli, including self-phosphatidylcholine (78) and Lp with immunomodulators exhibiting antitumoral activity (33, 77). Additionally, B1 cells coming from splenocytes could also proliferate under the effect of these Lp. Previous work by our group demonstrated that DPPC-containing Lp encapsulating OVA are internalized by B1 cells and elicit an increase in peritoneal lymphocytes (79, 80). Interestingly, empty DPPC Lp are able to reproduce the effect of those carrying only OVA (80, 81).

The selection of a suitable adjuvant for a therapeutic scenario, as occurs in cancer vaccines, has demands beyond the classical characteristics of an adjuvant for preventive vaccination. In this case, the induction of effective CTL activity is not easy to achieve in the tumor environment because of the variety of immunosuppressive strategies displayed by the tumor to restrict the effectiveness of antitumor responses (82). Despite this, an antitumoral response was observed in tumor-bearing mice treated with Lp/OVA/StII in contrast to those receiving Lp/OVA, reflecting additional properties associated with the former. Our data could suggest a capacity for Lp/OVA/StII to partially overcome the suppressing mechanisms generated by tumors, probably by combining the higher-quality CTL response with the influence on particular immune cells, as mentioned above.

Similar to other PFPs that can be activated by sulfhydryl groups (83), $_{rev}$StI W111C encapsulated into DPPC:Cho Lp was able to promote an Ag-specific CTL response equivalent to rStI (Fig. 7), probably as a consequence of its activation in the reducing environment of the endosomal compartment. In turn, organelle disruption by pore formation would lead to Ag delivery to cell cytosol (84). This finding shows that Lp containing $_{rev}$StI W111C could be a safer formulation, because they could only be activated after reaching the endosomal environment. Unexpectedly, $_{irrev}$StI W111C coencapsulated with OVA into DPPC:Cho Lp was able to induce an Ag-specific CTL response comparable to that observed with Lp carrying the wild-type protein rStI or its counterpart $_{rev}$StI W111C (Fig. 7), indicating that the pore-forming activity of Sts is not absolutely required for this outcome. In contrast, the effect of LLO incorporated into liposomal vesicles on the enhanced delivery of plasmid DNA was strictly correlated with the endo-somolytic activity of this PFP (85, 86).

Effective adjuvants should promote Ag delivery, as well as activate APCs (48). The recognition of bacterial PFPs by TLRs and the induction of APC maturation were documented (55). StII, although evolutionarily distant from bacterial PFPs, interacted with DCs, causing their activation in vitro (Fig. 8). Considering that partial leakage from Lp can occur in vivo as a consequence of their interaction with the biological medium (39, 60), free StII could be found at the inoculation site and initiate the activation of APCs located nearby. StII-containing Lp were not able to induce the maturation of DCs in vitro using serum-free medium (data not shown).

A Toll/TLR protein, as well as likely orthologs of key components of the TLR pathways, were found in anthozoan cnidarians, although the molecular nature of the ligands for these proteins is unknown (87). Actinoporins could be putative ligands for these Toll/TLR proteins, because vertebrate TLRs were suspected of binding to host molecules, including fibrinogen and heat shock proteins (88). StII could interact with other families of TLR proteins, such as those of vertebrates. This idea could account for the ability of StII to mature DCs as a pathogen-associated molecular pattern similar to bacterial PFPs, as well as explain the nonabsolute dependence between the pore-forming ability of Sts and their capacity to enhance an Ag-specific CTL response.

In conclusion, to our knowledge, this is the first report of an adjuvant based on StII encapsulated into Lp for the activation of a robust and functional CTL response with an antitumor effect in preventive and therapeutic scenarios, constituting a promising vaccine platform against cancer. Additionally, the nontotal dependence of the immunomodulatory effects of Sts on their pore-forming activity was demonstrated. The ability of StII to induce DC maturation in vitro might explain this particular behavior. The mechanisms conducive to DC activation and their relevance to the immunomodulatory properties of StII require further investigation.

Supplementary Material

Refer to Web version on PubMed Central for supplementary material.

Acknowledgments

We thank Gerardo Ramsés Hernández (Center for Genetic Engineering and Biotechnology, Havana, Cuba) for assistance with the lyophilization of Lp and Dr. Ignacio Hernández (Isotopes Centre, Havana, Cuba) for support with protein radiolabeling. We also thank Yanín Bebelagua and Armando López (CIM) for help with DC assays and excellent technical assistance with mice handling, respectively.

This work was supported by the Center of Molecular Immunology, the International Foundation for Science, and CAPES-MES Project No. 111/11. The David Rockefeller Center for Latin American Studies supported M.E.L.'s visit to Harvard Medical School.

Abbreviations used in this article

BMDC	bone marrow-derived DC
BMH	bis(maleimido)hexane
CF	carboxyfluorescein

Cho	cholesterol
CIM	Center of Molecular Immunology
DC	dendritic cell
DPPC	dipalmitoyl phosphatidylcholine
DRV	dehydration-rehydration vesicle
FSC	forward scatter
$_{irrev}$StI W111C	irreversibly inactive dimer of the mutant StI W111C
LLO	listeriolysin O
LN	lymph node
Lp	liposome
LUV	large unilamellar vesicle
OVA/PIC	OVA adjuvanted in PIC
PC	phosphatidylcholine
PFP	pore-forming protein
PIC	polyinosinic-polycytidylic acid
pmxB	polymyxin B
$_{rev}$StI W111C	reversibly inactive dimer of the mutant StI W111C stabilized by a disulfide bridge
rmGM-CSF	recombinant murine GM-CSF
rStI	recombinant StI
SM	sphingomyelin
St	sticholysin
tV	tumor volume
VSSP	very small size proteoliposome

References

1. Kaliński P, Schuitemaker JH, Hilkens CM, Kapsenberg ML. Prostaglandin E2 induces the final maturation of IL-12-deficient CD1a^{+}CD83^{+} dendritic cells: the levels of IL-12 are determined during the final dendritic cell maturation and are resistant to further modulation. J. Immunol. 1998; 161:2804–2809. [PubMed: 9743339]
2. Schiavoni G, Mattei F, Gabriele L. Type I interferons as stimulators of DC-mediated cross-priming: impact on anti-tumor response. Front. Immunol. 2013; 4:483. [PubMed: 24400008]

3. Banchereau J, Briere F, Caux C, Davoust J, Lebecque S, Liu YJ, Pulendran B, Palucka K. Immunobiology of dendritic cells. Annu. Rev. Immunol. 2000; 18:767–811. [PubMed: 10837075]
4. Kurts C, Robinson BWS, Knolle PA. Cross-priming in health and disease. Nat. Rev. Immunol. 2010; 10:403–414. [PubMed: 20498667]
5. Platzer B, Stout M, Fiebiger E. Antigen cross-presentation of immune complexes. Front. Immunol. 2014; 5:140. [PubMed: 24744762]
6. Nair S, Zhou F, Reddy R, Huang L, Rouse BT. Soluble proteins delivered to dendritic cells via pH-sensitive liposomes induce primary cytotoxic T lymphocyte responses in vitro. J. Exp. Med. 1992; 175:609–612. [PubMed: 1531064]
7. Paliwal SR, Paliwal R, Vyas SP. A review of mechanistic insight and application of pH-sensitive liposomes in drug delivery. Drug Deliv. 2015; 22:231–242. [PubMed: 24524308]
8. Christensen D, Korsholm KS, Andersen P, Agger EM. Cationic liposomes as vaccine adjuvants. Expert Rev. Vaccines. 2011; 10:513–521. [PubMed: 21506648]
9. Korsholm KS, Hansen J, Karlsen K, Filskov J, Mikkelsen M, Lindenstrøm T, Schmidt ST, Andersen P, Christensen D. Induction of $CD8^+$ T-cell responses against subunit antigens by the novel cationic liposomal CAF09 adjuvant. Vaccine. 2014; 32:3927–3935. [PubMed: 24877765]
10. Thomann JS, Heurtault B, Weidner S, Brayé M, Beyrath J, Fournel S, Schuber F, Frisch B. Antitumor activity of liposomal ErbB2/HER2 epitope peptide-based vaccine constructs incorporating TLR agonists and man-nose receptor targeting. Biomaterials. 2011; 32:4574–4583. [PubMed: 21474175]
11. Boks MA, Ambrosini M, Bruijns SC, Kalay H, van Bloois L, Storm G, Garcia-Vallejo JJ, van Kooyk Y. MPLA incorporation into DC-targeting glycoliposomes favours anti-tumour T cell responses. J. Control. Release. 2015; 216:37–46. [PubMed: 26151293]
12. Chikh GG, Kong S, Bally MB, Meunier JC, Schutze-Redelmeier MPM. Efficient delivery of Antennapedia homeodomain fused to CTL epitope with liposomes into dendritic cells results in the activation of $CD8^+$ T cells. J. Immunol. 2001; 167:6462–6470. [PubMed: 11714813]
13. Provoda CJ, Lee KD. Bacterial pore-forming hemolysins and their use in the cytosolic delivery of macromolecules. Adv. Drug Deliv. Rev. 2000; 41:209–221. [PubMed: 10699316]
14. Mandal M, Lee KD. Listeriolysin O-liposome-mediated cytosolic delivery of macromolecule antigen in vivo: enhancement of antigen-specific cytotoxic T lymphocyte frequency, activity, and tumor protection. Biochim. Biophys. Acta. 2002; 1563:7–17. [PubMed: 12007619]
15. Mandal M, Kawamura KS, Wherry EJ, Ahmed R, Lee KD. Cytosolic delivery of viral nucleoprotein by listeriolysin O-liposome induces enhanced specific cytotoxic T lymphocyte response and protective immunity. Mol. Pharm. 2004; 1:2–8. [PubMed: 15832496]
16. Andrews CD, Huh MS, Patton K, Higgins D, Van Nest G, Ott G, Lee KD. Encapsulating immunostimulatory CpG oligonucleotides in listeriolysin O-liposomes promotes a Th1-type response and CTL activity. Mol. Pharm. 2012; 9:1118–1125. [PubMed: 22376145]
17. Alvarez C, Mancheño JM, Martínez D, Tejuca M, Pazos F, Lanio ME. Sticholysins, two pore-forming toxins produced by the Caribbean Sea anemone *Stichodactyla helianthus*: their interaction with membranes. Toxicon. 2009; 54:1135–1147. [PubMed: 19268489]
18. Lanio ME, Morera V, Alvarez C, Tejuca M, Gómez T, Pazos F, Besada V, Martínez D, Huerta V, Padrón G, de los Angeles Chávez M. Purification and characterization of two hemolysins from *Stichodactyla helianthus*. Toxicon. 2001; 39:187–194. [PubMed: 10978735]
19. Huerta V, Morera V, Guanche Y, Chinea G, Gonzalez LJ, Betancourt L, Martínez D, Alvarez C, Lanio ME, Besada V. Primary structure of two cytolysin isoforms from *Stichodactyla helianthus* differing in their hemolytic activity. Toxicon. 2001; 39:1253–1256. [PubMed: 11306138]
20. Tejuca M, Dalla Serra M, Potrich C, Alvarez C, Menestrina G. Sizing the radius of the pore formed in erythrocytes and lipid vesicles by the toxin sticholysin I from the sea anemone *Stichodactyla helianthus*. J. Membr. Biol. 2001; 183:125–135. [PubMed: 11562794]
21. Tejuca M, Serra MD, Ferreras M, Lanio ME, Menestrina G. Mechanism of membrane permeabilization by sticholysin I, a cytolysin isolated from the venom of the sea anemone *Stichodactyla helianthus*. Biochemistry. 1996; 35:14947–14957. [PubMed: 8942660]

22. Martínez D, Otero A, Alvarez C, Pazos F, Tejuca M, Lanio ME, Gutiérrez-Aguirre I, Barlic A, Iloro I, Arrondo JL, et al. Effect of sphingomyelin and cholesterol on the interaction of St II with lipidic interfaces. Toxicon. 2007; 49:68–81. [PubMed: 17113118]
23. Pazos F, Valle A, Martínez D, Ramírez A, Calderón L, Pupo A, Tejuca M, Morera V, Campos J, Fando R, et al. Structural and functional characterization of a recombinant sticholysin I (rSt I) from the sea anemone *Stichodactyla helianthus*. Toxicon. 2006; 48:1083–1094. [PubMed: 17067649]
24. Pentón D, Pérez-Barzaga V, Díaz I, Reytor ML, Campos J, Fando R, Calvo L, Cilli EM, Morera V, Castellanos-Serra LR, et al. Validation of a mutant of the pore-forming toxin sticholysin-I for the construction of proteinase-activated immunotoxins. Protein Eng. Des. Sel. 2011; 24:485–493. [PubMed: 21296830]
25. Moore MW, Carbone FR, Bevan MJ. Introduction of soluble protein into the class I pathway of antigen processing and presentation. Cell. 1988; 54:777–785. [PubMed: 3261634]
26. Laemmli UK. Cleavage of structural proteins during the assembly of the head of bacteriophage T4. Nature. 1970; 227:680–685. [PubMed: 5432063]
27. Kirby C, Gregoriadis G. Dehydration-rehydration vesicles (DRV): a new method for high yield drug entrapment in liposomes. Biotechnology. 1984; 2:979–984.
28. Hunter WM, Greenwood FC. Preparation of iodine-131 labelled human growth hormone of high specific activity. Nature. 1962; 194:495–496. [PubMed: 14450081]
29. Martínez D, Campos AM, Pazos F, Álvarez C, Lanio ME, Casallanovo F, Schreier S, Salinas RK, Vergara C, Lissi E. Properties of St I and St II, two isotoxins isolated from *Stichodactyla helianthus*: a comparison. Toxicon. 2001; 39:1547–1560. [PubMed: 11478962]
30. Rouser G, Fkeischer S, Yamamoto A. Two dimensional then layer chromatographic separation of polar lipids and determination of phospholipids by phosphorus analysis of spots. Lipids. 1970; 5:494–496. [PubMed: 5483450]
31. Lutz MB, Kukutsch N, Ogilvie AL, Rössner S, Koch F, Romani N, Schuler G. An advanced culture method for generating large quantities of highly pure dendritic cells from mouse bone marrow. J. Immunol. Methods. 1999; 223:77–92. [PubMed: 10037236]
32. Basulto A, Casadelvalle I, Otero A, Pico MC. Sticholysin II, a cytolysin isolated from the Caribbean Sea anemone *Stichodactyla helianthus*, interacts with serum lipoproteins, Freund adjuvant and specific antibodies to this protein. Rev. Invest. Mar. 2006; 27:41–48.
33. Labrada M, Clavell M, Bebelagua Y, León Jd, Alonso DF, Gabri MR, Veloso RC, Vérez V, Fernández LE. Direct validation of NGcGM3 ganglioside as a new target for cancer immunotherapy. Expert Opin. Biol. Ther. 2010; 10:153–162. [PubMed: 20088712]
34. Lanio ME, Alvarez C, Martínez FD, Casallanovo F, Schreier S, Campos AM, Abuin E, Lissi E. Effect of a zwitterionic surfactant (HPS) on the conformation and hemolytic activity of St I and St II, two isotoxins purified from *Stichodactyla helianthus*. J. Protein Chem. 2002; 21:401–405. [PubMed: 12492150]
35. Lanio ME, Alvarez C, Pazos F, Martínez D, Martínez Y, Casallanovo F, Abuin E, Schreier S, Lissi E. Effects of sodium dodecyl sulfate on the conformation and hemolytic activity of St I and St II, two isotoxins purified from *Stichodactyla helianthus*. Toxicon. 2003; 41:65–70. [PubMed: 12467663]
36. Lanio ME, Alvarez C, Ochoa C, Ros U, Pazos F, Martínez D, Tejuca M, Eugenio LM, Casallanovo F, Dyszy FH, et al. Sticholysins I and II interaction with cationic micelles promotes toxins' conformational changes and enhanced hemolytic activity. Toxicon. 2007; 50:731–739. [PubMed: 17681582]
37. de los Ríos V, Mancheño JM, Lanio ME, Oñaderra M, Gavilanes JG. Mechanism of the leakage induced on lipid model membranes by the hemolytic protein sticholysin II from the sea anemone *Stichodactyla helianthus*. Eur. J. Biochem. 1998; 252:284–289. [PubMed: 9580155]
38. Frézard F. Liposomes: from biophysics to the design of peptide vaccines. Braz. J. Med. Biol. Res. 1999; 32:181–189. [PubMed: 10347753]
39. Ulrich AS. Biophysical aspects of using liposomes as delivery vehicles. Biosci. Rep. 2002; 22:129–150. [PubMed: 12428898]
40. Stevens L. Egg white proteins. Comp. Biochem. Physiol. B. 1991; 100:1–9. [PubMed: 1756612]

41. Keene JA, Forman J. Helper activity is required for the in vivo generation of cytotoxic T lymphocytes. J. Exp. Med. 1982; 155:768–782. [PubMed: 6801178]
42. Schoenberger SP, Toes REM, van der Voort EIH, Offringa R, Melief CJM. T-cell help for cytotoxic T lymphocytes is mediated by CD40-CD40L interactions. Nature. 1998; 393:480–483. [PubMed: 9624005]
43. Feau S, Garcia Z, Arens R, Yagita H, Borst J, Schoenberger SP. The $CD4^+$ T-cell help signal is transmitted from APC to $CD8^+$ T-cells via CD27-CD70 interactions. Nat. Commun. 2012; 3:948. [PubMed: 22781761]
44. Williams MA, Bevan MJ. Effector and memory CTL differentiation. Annu. Rev. Immunol. 2007; 25:171–192. [PubMed: 17129182]
45. Qiu F, Cui Z. $CD4^+$ T helper cell response is required for memory in $CD8^+$ T lymphocytes induced by a poly(I:C)-adjuvanted MHC I-restricted peptide epitope. [Published erratum appears in 2007 J. Immunother. 30: 576.]. J. Immunother. 2007; 30:180–189. [PubMed: 17471165]
46. Mesa C, de León J, Fernández LE. Very small size proteoliposomes derived from *Neisseria meningitidis*: an effective adjuvant for generation of CTL responses to peptide and protein antigens. Vaccine. 2006; 24:2692–2699. [PubMed: 16316710]
47. Gregoriadis G. The immunological adjuvant and vaccine carrier properties of liposomes. J. Drug Target. 1994; 2:351–356. [PubMed: 7704478]
48. Perrie Y, Crofts F, Devitt A, Griffiths HR, Kastner E, Nadella V. Designing liposomal adjuvants for the next generation of vaccines. Adv. Drug Deliv. Rev. 2016; 99(Pt. A):85–96. [PubMed: 26576719]
49. Mazumdar T, Anam K, Ali N. A mixed Th1/Th2 response elicited by a liposomal formulation of Leishmania vaccine instructs Th1 responses and resistance to Leishmania donovani in susceptible BALB/c mice. Vaccine. 2004; 22:1162–1171. [PubMed: 15003644]
50. Luzardo MC, Calderón L, Martínez Y, Labrada A, Facenda E, Alvarez CM, Pazos IF, de León J, Alonso ME, Lanio ME. Liposomal lipids as immunoadjuvants for recombinant human epidermal growth factor (rhEGF) and the main allergens (maDer s) of the *Dermatophagoides siboney* dust mite. Biotecnol. Apl. 2006; 23:330–343.
51. Beck Z, Matyas GR, Jalah R, Rao M, Polonis VR, Alving CR. Differential immune responses to HIV-1 envelope protein induced by liposomal adjuvant formulations containing monophosphoryl lipid Awith or without QS21. Vaccine. 2015; 33:5578–5587. [PubMed: 26372857]
52. García-Linares S, Castrillo I, Bruix M, Menéndez M, Alegre-Cebollada J, Martínez-del-Pozo Á, Gavilanes JG. Three-dimensional structure of the actinoporin sticholysin I. Influence of long-distance effects on protein function. Arch. Biochem. Biophys. 2013; 532:39–45. [PubMed: 23376038]
53. Valle A, López-Castilla A, Pedrera L, Martínez D, Tejuca M, Campos J, Fando R, Lissi E, Alvarez C, Lanio ME, et al. Cys mutants in functional regions of Sticholysin I clarify the participation of these residues in pore formation. Toxicon. 2011; 58:8–17. [PubMed: 21510967]
54. Antonini V, Pérez-Barzaga V, Bampi S, Pentón D, Martínez D, Dalla Serra M, Tejuca M. Functional characterization of sticholysin I and W111C mutant reveals the sequence of the actinoporin's pore assembly. PLoS One. 2014; 9:e110824. [PubMed: 25350457]
55. Park JM, Ng VH, Maeda S, Rest RF, Karin M. Anthrolysin O and other gram-positive cytolysins are toll-like receptor 4 agonists. J. Exp. Med. 2004; 200:1647–1655. [PubMed: 15611291]
56. Morón G, Dadaglio G, Leclerc C. New tools for antigen delivery to the MHC class I pathway. Trends Immunol. 2004; 25:92–97. [PubMed: 15102368]
57. Weber DK, Yao S, Rojko N, Anderluh G, Lybrand TP, Downton MT, Wagner J, Separovic F. Characterization of the lipid-binding site of equinatoxin II by NMR and molecular dynamics simulation. Biophys. J. 2015; 108:1987–1996. [PubMed: 25902438]
58. Barlic A, Gutiérrez-Aguirre I, Caaveiro JMM, Cruz A, Ruiz-Argüuello MB, Pérez-Gil J, González-Mañas JM. Lipid phase coexistence favors membrane insertion of equinatoxin-II, a pore-forming toxin from Actinia equina. J. Biol. Chem. 2004; 279:34209–34216. [PubMed: 15175339]
59. Pedrera L, Gomide AB, Sánchez RE, Ros U, Wilke N, Pazos F, Lanio ME, Itri R, Fanani ML, Alvarez C. The presence of sterols favors sticholysin I-membrane association and pore formation

regardless of their ability to form laterally segregated domains. Langmuir. 2015; 31:9911–9923. [PubMed: 26273899]

60. Lanio ME, Luzardo MC, Laborde R, Sánchez O, Cruz-Leal Y, Pazos F, Tejuca M, Valle A, Alonso ME, Fernández LE, Alvarez C. Las vesículas liposomales: obtención, propiedades y aplicaciones potenciales en la biomedicina. Rev. Cub. Física. 2009; 26:23–30.
61. Karmakar S, Raghunathan VA. Structure of phospholipid-cholesterol membranes: an x-ray diffraction study. Phys. Rev. E Stat. Nonlin. Soft Matter Phys. 2005; 71:061924. [PubMed: 16089782]
62. Shah RR, O'Hagan DT, Amiji MM, Brito LA. The impact of size on particulate vaccine adjuvants. Nanomedicine (Lond.). 2014; 9:2671–2681. [PubMed: 25529570]
63. Henriksen-Lacey M, Devitt A, Perrie Y. The vesicle size of DDA: TDB liposomal adjuvants plays a role in the cell-mediated immune response but has no significant effect on antibody production. J. Control. Release. 2011; 154:131–137. [PubMed: 21640145]
64. Nordly P, Agger EM, Andersen P, Nielsen HM, Foged C. Incorporation of the TLR4 agonist monophosphoryl lipid A into the bilayer of DDA/TDB liposomes: physico-chemical characterization and induction of $CD8^+$ T-cell responses in vivo. Pharm. Res. 2011; 28:553–562. [PubMed: 21042837]
65. Oehen S, Brduscha-Riem K. Differentiation of naive CTL to effector and memory CTL: correlation of effector function with phenotype and cell division. J. Immunol. 1998; 161:5338–5346. [PubMed: 9820507]
66. Jackson SS, Schmitz JE, Kuroda MJ, McKay PF, Sumida SM, Martin KL, Yu F, Lifton MA, Gorgone DA, Letvin NL. Evaluation of CD62L expression as a marker for vaccine-elicited memory cytotoxic T lymphocytes. Immunology. 2005; 116:443–453. [PubMed: 16313358]
67. Leignadier J, Labrecque N. Epitope density influences $CD8^+$ memory T cell differentiation. PLoS One. 2010; 5:e13740. [PubMed: 21060788]
68. Dietrich G, Hess J, Gentschev I, Knapp B, Kaufmann SH, Goebel W. From evil to good: a cytolysin in vaccine development. Trends Microbiol. 2001; 9:23–28. [PubMed: 11166239]
69. Walls ZF, Goodell S, Andrews CD, Mathis J, Lee KD. Mutants of listeriolysin O for enhanced liposomal delivery of macromolecules. J. Biotechnol. 2013; 164:500–502. [PubMed: 23416330]
70. Asano K, Nabeyama A, Miyake Y, Qiu CH, Kurita A, Tomura M, Kanagawa O, Fujii S, Tanaka M. CD169-positive macrophages dominate antitumor immunity by crosspresenting dead cell-associated antigens. Immunity. 2011; 34:85–95. [PubMed: 21194983]
71. La Gruta NL, Rothwell WT, Cukalac T, Swan NG, Valkenburg SA, Kedzierska K, Thomas PG, Doherty PC, Turner SJ. Primary CTL response magnitude in mice is determined by the extent of naive T cell recruitment and subsequent clonal expansion. J. Clin. Invest. 2010; 120:1885–1894. [PubMed: 20440073]
72. Arens R, Schoenberger SP. Plasticity in programming of effector and memory CD8 T-cell formation. Immunol. Rev. 2010; 235:190–205. [PubMed: 20536564]
73. Zloza A, Kohlhapp FJ, Lyons GE, Schenkel JM, Moore TV, Lacek AT, O'Sullivan JA, Varanasi V, Williams JW, Jagoda MC, et al. NKG2D signaling on $CD8^+$ T cells represses T-bet and rescues CD4-unhelped $CD8^+$ T cell memory recall but not effector responses. Nat. Med. 2012; 18:422–428. [PubMed: 22366950]
74. Taneichi M, Tanaka Y, Kakiuchi T, Uchida T. Liposome-coupled peptides induce long-lived memory CD8 T cells without CD4 T cells. PLoS One. 2010; 5:e15091. [PubMed: 21264321]
75. Yoshikawa T, Okada N, Tsujino M, Gao JQ, Hayashi A, Tsutsumi Y, Mayumi T, Yamamoto A, Nakagawa S. Vaccine efficacy of fusogenic liposomes containing tumor cell-lysate against murine B16BL6 melanoma. Biol. Pharm. Bull. 2006; 29:100–104. [PubMed: 16394519]
76. Sakurai Y, Hatakeyama H, Sato Y, Akita H, Takayama K, Kobayashi S, Futaki S, Harashima H. Endosomal escape and the knockdown efficiency of liposomal-siRNA by the fusogenic peptide shGALA. Biomaterials. 2011; 32:5733–5742. [PubMed: 21605898]
77. Kim DH, Moon C, Oh SS, Park S, Jeong JW, Kim S, Lee HG, Kwon HJ, Kim KD. Liposome-encapsulated CpG enhances antitumor activity accompanying the changing of lymphocyte populations in tumor via intratumoral administration. Nucleic Acid Ther. 2015; 25:95–102. [PubMed: 25692533]

78. Giabbai B, Sidobre S, Crispin MD, Sanchez-Ruíz Y, Bachi A, Kronenberg M, Wilson IA, Degano M. Crystal structure of mouse CD1d bound to the self ligand phosphatidylcholine: a molecular basis for NKT cell activation. J. Immunol. 2005; 175:977–984. [PubMed: 16002697]

79. Cruz-Leal Y, Machado Y, López-Requena A, Canet L, Laborde R, Álvares AM, Lucatelli Laurindo MF, Santo Tomas JF, Alonso ME, Alvarez C, et al. Role of B-1 cells in the immune response against an antigen encapsulated into phosphatidylcholine-containing liposomes. Int. Immunol. 2014; 26:427–437. [PubMed: 24618118]

80. Cruz-Leal Y, Lucatelli Laurindo MF, Osugui L, Luzardo Mdel C, López-Requena A, Alonso ME, Álvarez C, Popi AF, Mariano M, Pérez R, Lanio ME. Liposomes of phosphatidylcholine and cholesterol induce an M2-like macrophage phenotype reprogrammable to M1 pattern with the involvement of B-1 cells. Immunobiology. 2014; 219:403–415. [PubMed: 24594322]

81. Cruz-Leal Y, López-Requena A, Lopetegui-González I, Machado Y, Alvarez C, Pérez R, Lanio ME. Phosphocholine-specific antibodies improve T-dependent antibody responses against OVA encapsulated into phosphatidylcholine-containing liposomes. Front. Immunol. 2016; 7:374. [PubMed: 27713745]

82. Rabinovich GA, Gabrilovich D, Sotomayor EM. Immunosuppressive strategies that are mediated by tumor cells. Annu. Rev. Immunol. 2007; 25:267–296. [PubMed: 17134371]

83. Palmer M. The family of thiol-activated, cholesterol-binding cytolysins. Toxicon. 2001; 39:1681–1689. [PubMed: 11595631]

84. Saito G, Swanson JA, Lee KD. Drug delivery strategy utilizing conjugation via reversible disulfide linkages: role and site of cellular reducing activities. Adv. Drug Deliv. Rev. 2003; 55:199–215. [PubMed: 12564977]

85. Lorenzi GL, Lee KD. Enhanced plasmid DNA delivery using anionic LPDII by listeriolysin O incorporation. J. Gene Med. 2005; 7:1077–1085. [PubMed: 15776501]

86. Kullberg M, McCarthy R, Anchordoquy TJ. Gene delivery to Her-2+ breast cancer cells using a two-component delivery system to achieve specificity. Nanomedicine (Lond.). 2014; 10:1253–1262.

87. Hemmrich G, Miller DJ, Bosch TCG. The evolution of immunity: a low-life perspective. Trends Immunol. 2007; 28:449–454. [PubMed: 17855167]

88. Beg AA. Endogenous ligands of Toll-like receptors: implications for regulating inflammatory and immune responses. Trends Immunol. 2002; 23:509–512. [PubMed: 12401394]

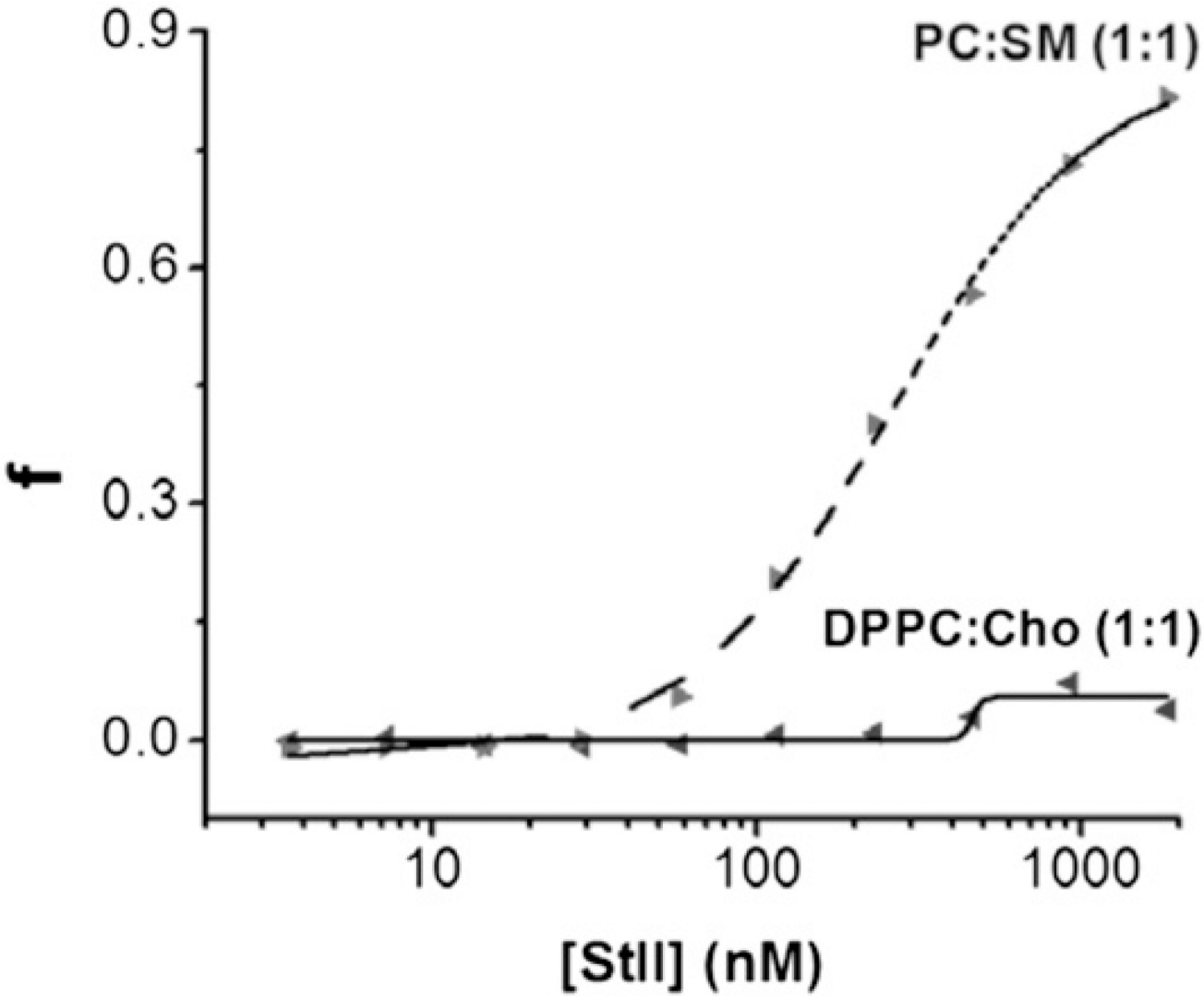

FIGURE 1.

StII does not show permeabilizing activity on liposomal vesicles composed of DPPC:Cho (1:1). LUVs comprising DPPC:Cho or PC:SM (1:1 molar ratio) encapsulating CF were exposed at different StII concentrations (2.5–1400 nM). LUVs were diluted in 10 mM Tris-HCl, 140 mM NaCl (pH 7.4) to reach a final lipid concentration of 0.2 μM. Vesicles of PC:SM were used as positive control. Excitation wavelength: 490 nm. Emission wavelength: 520 nm. The experiments were carried out at room temperature. The fraction of permeabilized vesicles (*f*) at a fixed time was estimated as: $f = (F_f - F_0)/(F_{max} - F_0)$, considering that release of fluorescent probe is simultaneous to pore formation, where F_0 and F_f are fluorescence values before and after adding StII, respectively, and F_{max} is the fluorescence measured in the presence of 0.1% Triton X-100. Data are from a single experiment representative of two independent experiments.

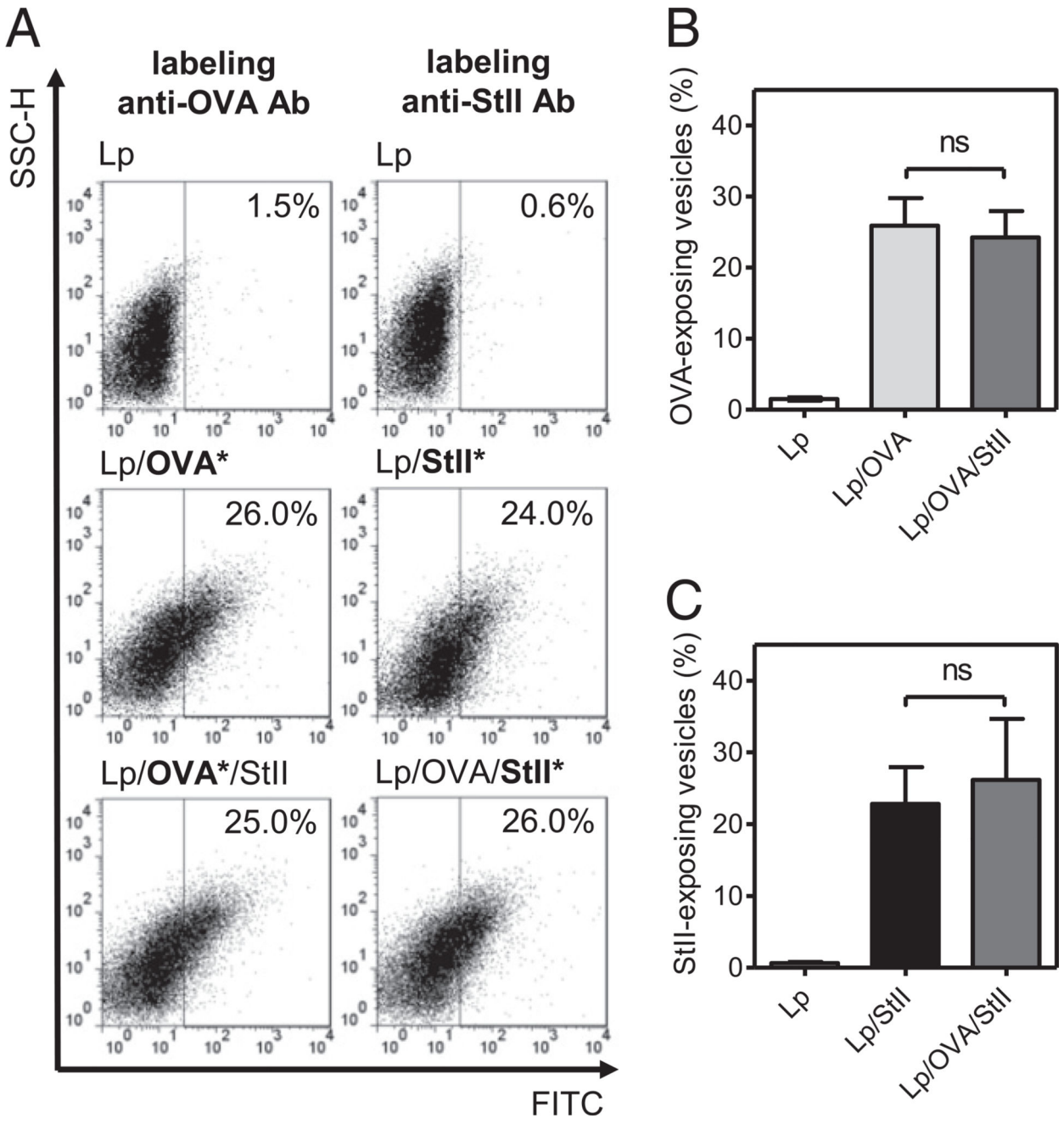

FIGURE 2.

Presence of OVA and StII on the surface of DPPC:Cho Lp. Freshly prepared DRVs of DPPC:Cho (1:1) empty (Lp), encapsulating OVA (Lp/OVA), and encapsulating StII with or without OVA (Lp/OVA/StII, Lp/StII) were incubated with polyclonal Abs from mice and rabbit specific to OVA or StII, respectively. Subsequently, vesicles were treated with an FITC-conjugated Ab anti-mouse IgG or an FITC-conjugated anti-rabbit IgG and examined by flow cytometry. (**A**) A representative side scatter-area (SSC-H) versus FITC–anti-IgG dot plot graph of each formulation is shown. Asterisks indicate the protein assessed in each case. Mean (± SD) vesicle percentage from different liposomal preparations ($n = 6$) exposing OVA

(**B**) or StII (**C**) at the surface. No significant differences (ns) were detected according to the two-tailed unpaired *t* test ($p > 0.05$). Data shown are from a single experiment representative of two experiments yielding comparable results.

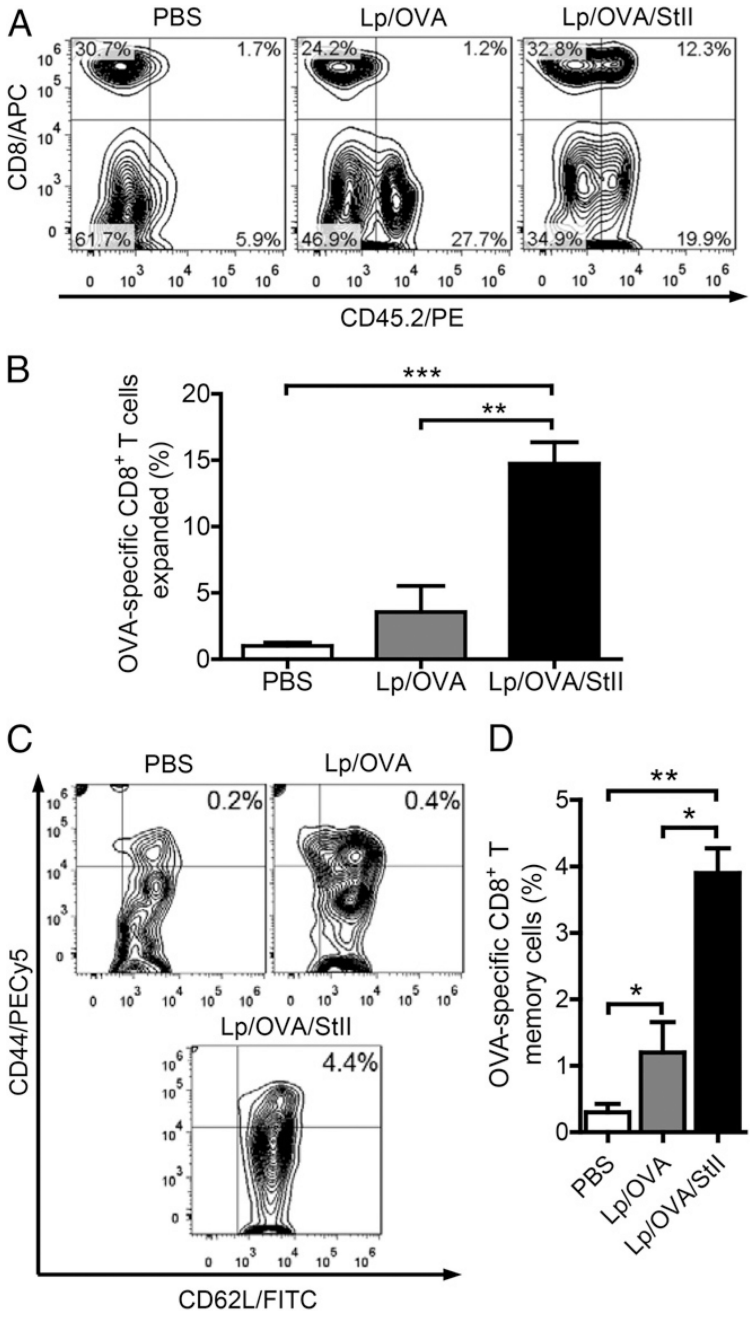

FIGURE 3.

Immunization with StII coencapsulated into the DPPC:Cho Lp with OVA induces significant expansion of OVA-specific $CD8^+$ T lymphocytes. Splenocytes (25×10^6 equivalent to 5.5×10^6 OVA-specific $CD8^+$ T cells) from OT-1 mice ($CD45.2^+$) were transferred i.v. into Ly5 mice ($CD45.1^+$). Two days later, Ly5 mice ($n = 3$) were immunized s.c. twice (12-d interval) with Lp/OVA/StII (50 μg OVA and 6.25 μg StII), Lp/OVA (50 μg OVA), or PBS (as negative control). Seven days after the second immunization, the inguinal LN closest to the inoculation site of each mouse was removed and homogenized, and $CD8^+$ $CD45.2^+$ cells were analyzed by flow cytometry. (**A**) Each contour graph, with the respective cell

percentages in each quadrant referred to the lymphocyte gate, corresponds to an individual animal representative of each group. (**B**) Percentage (mean ± SEM) of $CD8^+$ $CD45.2^+$ cells for each treatment. (**C**) Contour graphs showing the percentage of $CD44^{high}$ $CD62L^+$ cells ($CD8^+$ memory cells) in relation to the lymphocyte gate of an individual mouse representative of each immunized group. Graphs are from the $CD8^+$ $CD45.2^+$ gate. (D) Percentage (mean ± SEM) of $CD44^{high}$ $CD62L^+$ cells for each group. Data in (B) and (D) are from a meta-analysis of two independent assays. $*p < 0.05$, $**p < 0.01$, $***p < 0.001$, two-tailed unpaired *t* test.

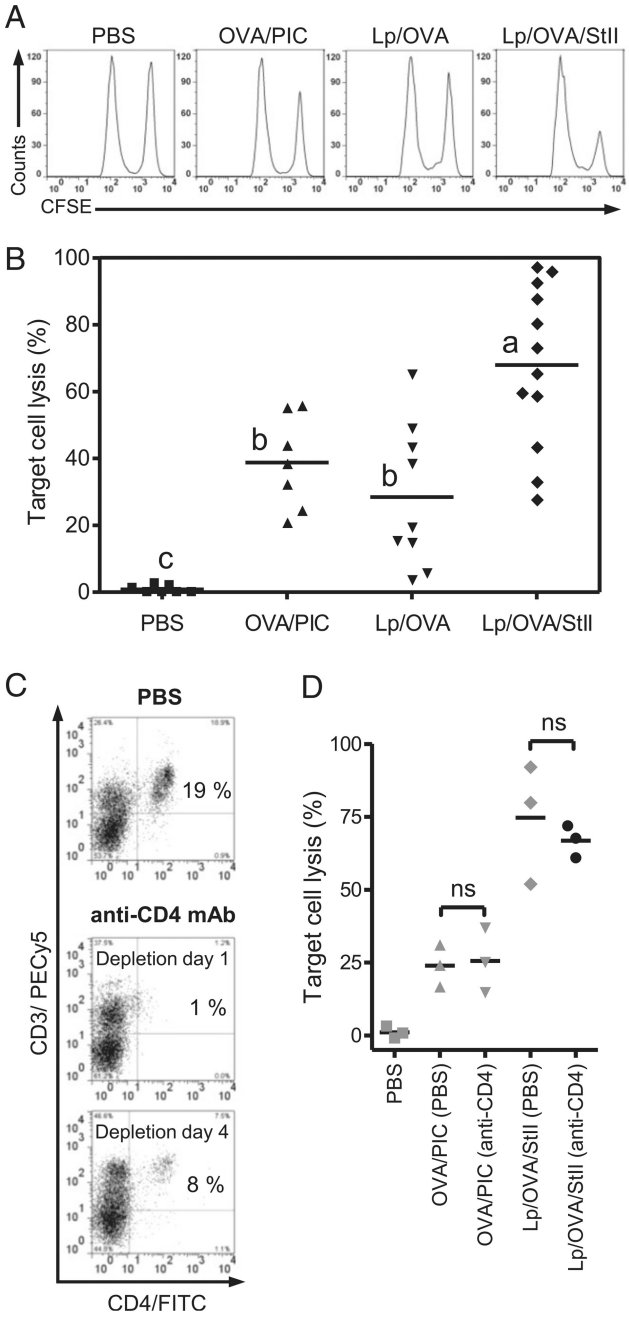

FIGURE 4.

Inclusion of StII into DPPC:Cho Lp containing OVA enhances OVA-specific cytotoxic response in mice. C57BL/6 mice ($n = 3$) were immunized s.c. twice at days 0 and 12 with Lp/OVA (50 μg OVA) or Lp/OVA/StII (50 μg OVA and 6.25 μg StII). PBS and 1 mg of OVA mixed with 100 μg PIC (OVA/PIC) were injected into mice as negative and positive controls, respectively. Eight days after the second immunization, mice received 60×10^6 cells containing a 1:1 proportion of target cells (SIINFEKL-charged and $CFSE^{bright}$-labeled splenocytes) and control cells (without peptide and $CFSE^{dull}$-labeled splenocytes) i.v., and mice were sacrificed 16–18 h later. Inguinal draining LNs were harvested, and the total

events corresponding to both fluorescent intensities ($CFSE^{dull}$ and $CFSE^{bright}$) were determined by FACS. The percentage of specific lysis was calculated as 100 ($CFSE^{bright}$/$CFSE^{dull}$)$_{vaccinated}$ × 100 × ($CFSE^{dull}$/$CFSE^{bright}$)$_{PBS}$. (**A**) Line graphs of $CFSE^{dull}$ and $CFSE^{bright}$ cells from an individual mouse representative of each experimental group. (**B**) Percentages of target cell lysis in individual animals from multiple in vivo CTL assays; the average value is represented by a horizontal line. Different letters indicate significant differences among groups based on the Dunnett T3 test (*p* values are specified in the *Results*). In other similar CTL assays, mice immunized with Lp/OVA/StII and OVA/PIC were injected i.p. with an anti-CD4 mAb or PBS as control, at 4-d intervals, starting at day −1. (**C**) Dot plot graphs of CD4 versus CD3 of splenocytes from individual mice receiving anti-CD4 mAb or PBS at days 1 and 4 after treatment. Quadrants were individually set at positions where unstained cells signals were <1%. Values correspond to the percentage of cells in relation to the total lymphocytes in spleens. (**D**) Each data point represents cytotoxic activity in individual experimental mice. (anti-CD4) and (PBS) indicate animal groups receiving anti-CD4 mAb or PBS, respectively. Statistical significance was calculated using a two-tailed unpaired *t* test. The figure shows one representative experiment from three repetitions with similar results. ns, not significant, $p > 0.05$.

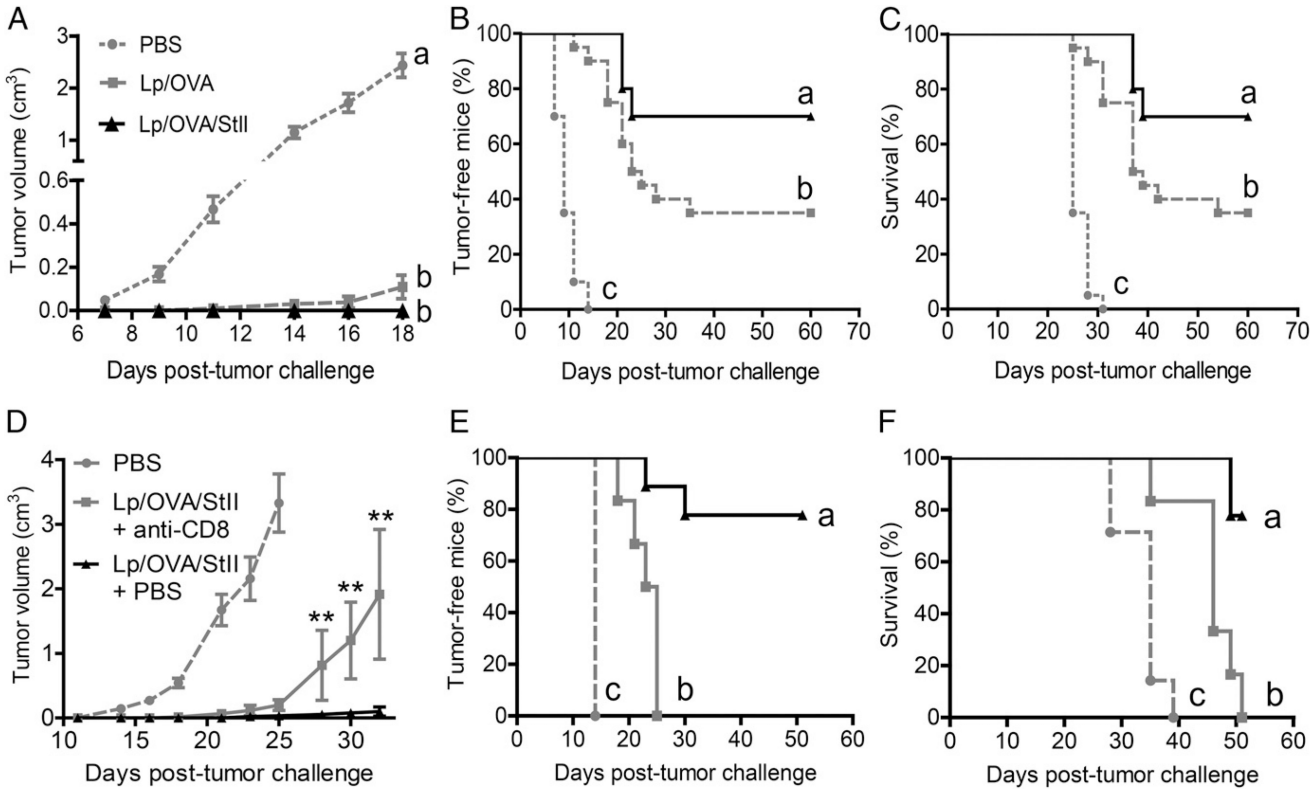

FIGURE 5.

StII coencapsulated into DPPC:Cho Lp with the Ag induces remarkable antitumor prophylactic immunity that decreases upon depletion of $CD8^+$ T lymphocytes. C57BL/6 mice were immunized i.m. twice with Lp/OVA (50 μg OVA) or Lp/OVA/StII (50 μg OVA and 6.25 μg StII) on days 0 and 12. Mice were challenged 7 d later with 3×10^5 cells E.G7-OVA tumor cells. A group of mice received PBS as control. Time courses of tV increase (mean ± SEM) (**A**), tumor grafting (**B**), and survival curves (**C**) in experimental groups after tumor challenge. Data are representatives of three independent experiments, each including 7–10 mice per group. Different letters indicate statistical differences among groups based on the Dunnett T3 test (A) and the log-rank test (B and C). The *p* values are specified in the *Results*. In another similar antitumoral assay, but immunizing s.c. only with Lp/OVA/StII (OVA 50 μg), mice were depleted of $CD8^+$ T cells by i.p. injection of anti-CD8 mAb (1 mg/mice) 1 d before tumor challenge or they received PBS instead of anti-CD8 (nondepleted group). Time courses of tV increase (mean ± SEM) (**D**), tumor grafting (**E**), and survival curves (F) of experimental groups. Statistically significant differences were estimated by the Mann–Whitney *U* test between the mice groups depleted or not of $CD8^+$ T lymphocytes (D) and the log-rank test (E and F). Different letters indicate statistical differences among groups (*p* values are specified in the *Results*). Two experiments were performed with similar results. $^{**}p < 0.01$.

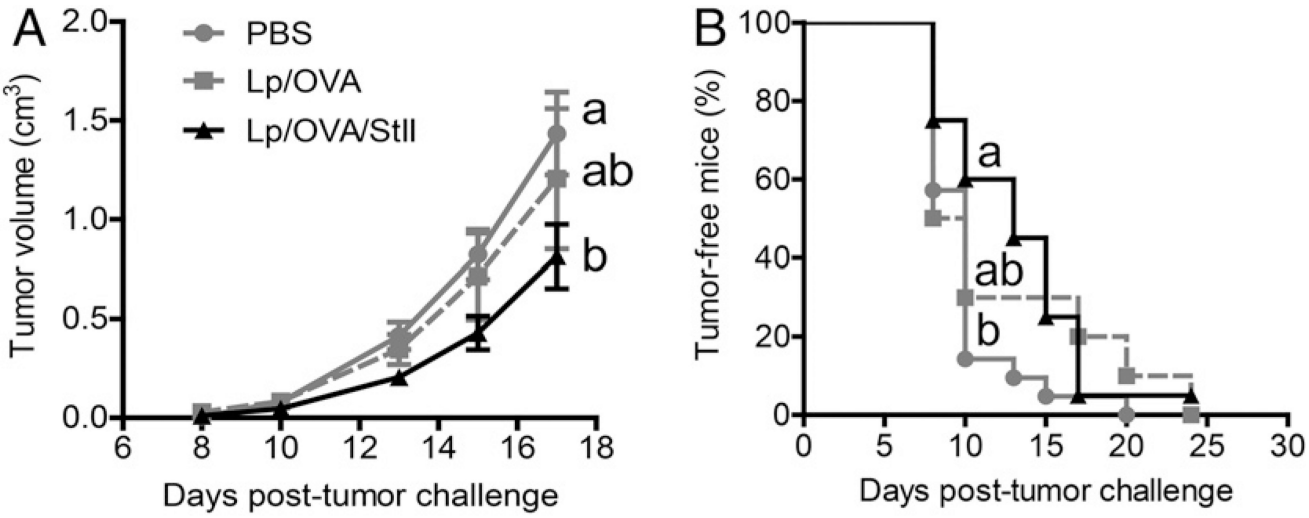

FIGURE 6.

StII coencapsulated into DPPC:Cho Lp with the Ag elicits a therapeutic antitumoral response. The antitumor therapeutic assay was carried out by challenging the mice ($n = 10$) with an E.G7-OVA tumor 3 d before immunization. Animals were injected s.c. once per week with Lp/OVA/StII or Lp/OVA (OVA 50 μg) three times. The control group was treated with PBS. Time courses of the tV increase (mean ± SEM) (**A**) and tumor grafting (**B**). Different letters indicate statistical differences among groups based on the Dunn test (A) or the log-rank test (B). The p values are specified in the *Results*. Data represent the result from a meta-analysis of three independent experiments.

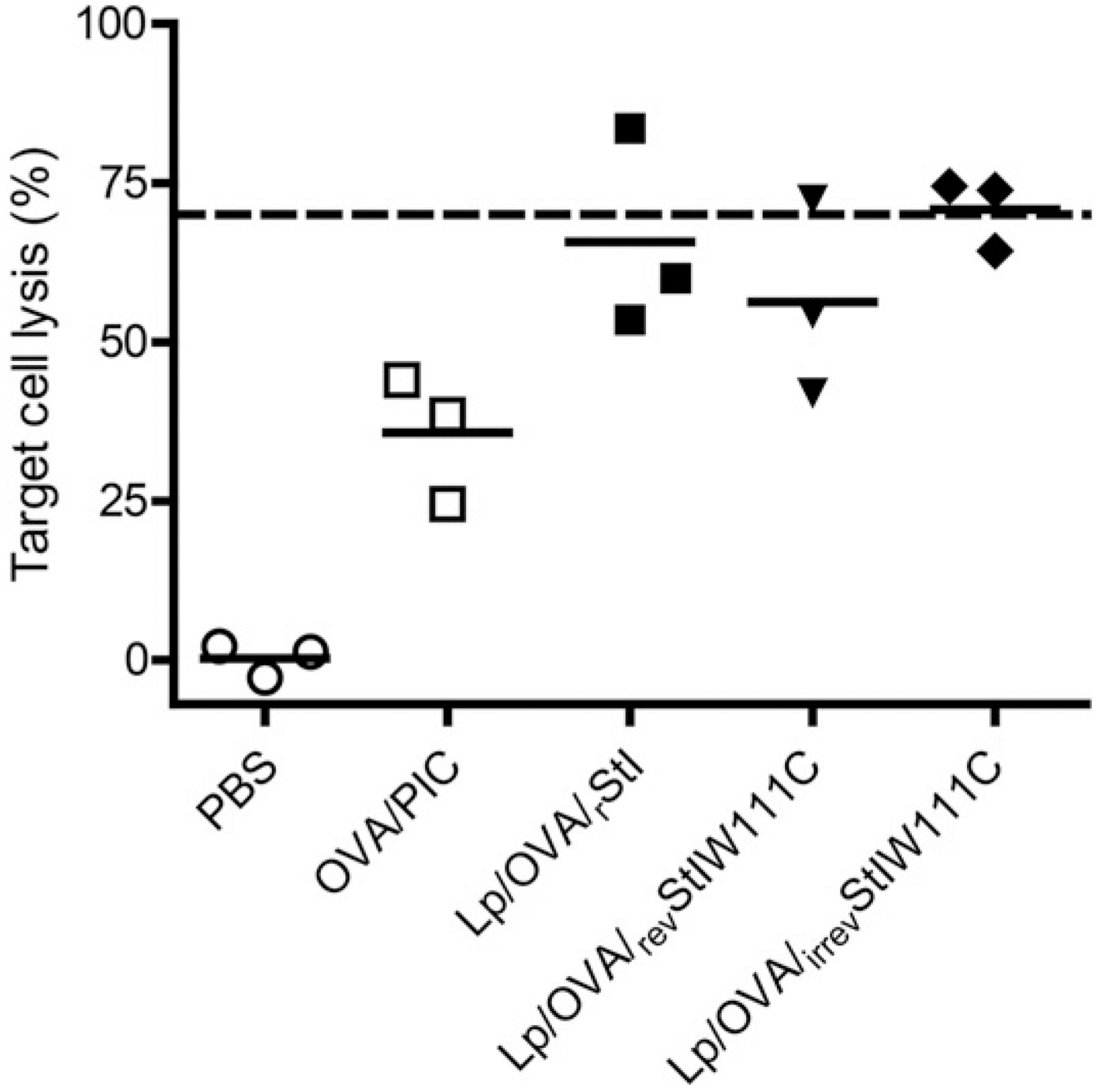

FIGURE 7.

An irreversibly inactive dimer of rStI coencapsulated into DPPC:Cho Lp with OVA induces a similar Ag-specific cytotoxicity as StII-containing Lp. C57BL/6 mice (three mice per group) were immunized s.c. twice with OVA/PIC (1 mg of OVA, 100 μg of PIC) or with Lp/OVA/Sts (rStI, $_{rev}$StI W111C, or $_{irrev}$StI W111C) (50 μg of OVA and 6.25 μg of St) on days 0 and 12. A group of mice received PBS as control. The CTL assay was performed in vivo as described in Fig. 4. Each data point and the horizontal solid lines represent the cytotoxic activity of individual mice and the average values, respectively. The dashed line

indicates the average lysis (%) from animals immunized with Lp/OVA/StII (Fig. 4). Data are from one representative experiment of two independent sets with similar results.

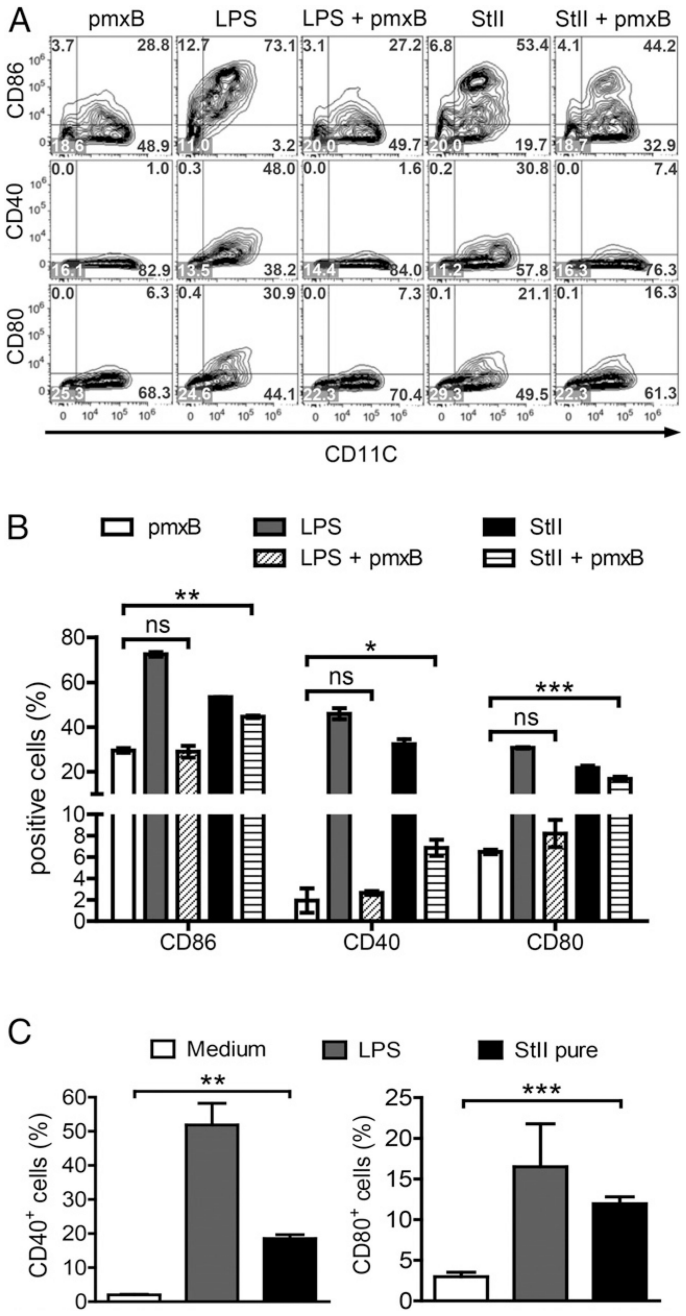

FIGURE 8.

StII promotes DC maturation in vitro, independent of the presence of contaminating LPS. Immature BMDCs were obtained from femurs and tibias of C57BL/.6 mice. After 7 d of culture, cells were harvested, counted, and seeded again at 1×10^6 cells per milliliter. StII (1 μg/ml) was added to immature BMDCs in 2 ml of serum-free medium for 3 h, and the PFP was subsequently inactivated by the addition of 10% FCS. LPS (1 μg/ml), LPS plus pmxB (10 μg/ml), StII plus pmxB, and StII free of endotoxin by column purification (pure StII) were also assayed under similar conditions. Eighteen hours later, the upregulation of costimulatory molecules on the BMDC surface was detected by flow cytometry. Doublets

were excluded from total acquired cells according to FSC profiles (FSC-area versus FSC-high), and the percentages of DCs ($CD11c^+$ cells) expressing costimulatory molecules were analyzed on gated live cells. (**A**) Contour graphs representative of the expression of CD86, CD40, and CD80 costimulatory molecules by $CD11c^+$ cells. Values in the quadrants represent cell percentages. (**B** and **C**) Percentages of $CD11c^+$ cells expressing each costimulatory molecule (mean ± SD). Data are from one representative experiment of three independent assays with similar results; each one was performed at least in duplicate. *$p < 0.05$, **$p < 0.01$, ***$p < 0.001$. ns, not significant.